A Comprehensive Land-Use/Hydrological Modeling System for Scenario Simulations in the Elbow River Watershed, Alberta, Canada

**Gayan Nishad Wijesekara · Babak Farjad ·
Anil Gupta · Ying Qiao · Patrick Delaney ·
Danielle J. Marceau**

Abstract The Elbow River watershed in Alberta covers an area of 1,238 km^2 and represents an important source of water for irrigation and municipal use. In addition to being located within the driest area of southern Canada, it is also subjected to considerable pressure for land development due to the rapid population growth in the City of Calgary. In this study, a comprehensive modeling system was developed to investigate the impact of past and future land-use changes on hydrological processes considering the complex surface–groundwater interactions existing in the watershed. Specifically, a spatially explicit land-use change model was coupled with MIKE SHE/MIKE 11, a distributed physically based catchment and channel flow model. Following a rigorous sensitivity analysis along with the calibration and validation of these models, four land-use change scenarios were simulated from 2010 to 2031: business as usual (BAU), new development concentrated within the Rocky View County (RV-LUC) and in Bragg Creek (BC-LUC), respectively, and development based on projected population growth (P-LUC). The simulation results reveal that the rapid urbanization and deforestation create an increase in overland flow, and a decrease in evapotranspiration (ET), baseflow, and infiltration mainly in the east sub-catchment of the watershed. The land-use scenarios affect the hydrology of the watershed differently. This study is the most comprehensive investigation of its nature done so far in the Elbow River watershed. The results obtained are in accordance with similar studies conducted in Canadian contexts. The proposed modeling system represents a unique and flexible framework for investigating a variety of water related sustainability issues.

Keywords Hydrological modeling · Land-use change · MIKE SHE · MIKE 11 · Cellular automata · Elbow River watershed · Surface–groundwater interactions

Introduction

The transformation of earth's land surface has many consequences for biophysical systems at all scales ranging from local urban heat islands and modifications in stream flow patterns to altered patterns of global atmospheric circulation and long-term extinction of species. Understanding the consequences of land-use change for hydrological processes, such as changes in water demand and supply from altered hydrological processes of infiltration and groundwater recharge and runoff, and integrating this understanding into the emerging focus on land-change science has been recognized as a major need (DeFries and Eshleman 2004).

Canada has an extensive reserve of freshwater, which is, therefore, often taken for granted (Coote and Gregorich 2000). However, in some places in Canada, water is scarce, such as in the Western Prairie Provinces (WPP), an area 1/5 of the size of Europe. Lying in the rain shadow of the Rocky Mountains, the WPP are considered the driest area of southern Canada (Coote and Gregorich 2000; Schindler and Donahue 2006). Among the major rivers in the WPP,

G. N. Wijesekara (✉) · B. Farjad · D. J. Marceau
Department of Geomatics Engineering, University of Calgary,
Calgary, AB, Canada
e-mail: axlrnish@yahoo.com

A. Gupta
Alberta Environment and Sustainable Resource Development,
Calgary, AB, Canada

Y. Qiao · P. Delaney
DHI Water and Environment Canada, Cambridge, ON, Canada

there has been a moderate decline in the total annual stream flows over the twentieth century (Gan 2000; Rood et al. 2005; Chen et al. 2006; Rood et al. 2008; Shepherd et al. 2010), while the summer flows have declined significantly. Worst affected is the South Saskatchewan River with a reduction of summer flows by 84% since the early 1900s. The Oldman, Bow, which Elbow is part of, and Red Deer Rivers contribute to the South Saskatchewan River and have been subjected to increased withdrawals to variable land-use activities such as irrigation, and municipal and industrial uses. All of these tributaries flow through semi-arid and sub-humid ecozones. The Elbow River watershed in southern Alberta is one of the catchments in the WPP that is critically affected. Designing an adequate modeling approach to investigate the impact of past and future land-use changes on the hydrology of this watershed has become an urgent challenge considering its significance for the population living in that region.

In previous studies conducted to evaluate the impact of land-use changes on hydrological processes, scientists have attempted to use both conceptual/semi-distributed or lumped (Fohrer et al. 2005; Thanapakpawin et al. 2006; Lin et al. 2007; Hurkmans et al. 2009), and physically/distributed (Niehoff et al. 2002; Oogathoo 2006; Chu et al. 2010; Wijesekara et al. 2012) modeling approaches. Fohrer et al. (2005) evaluated the impact of different average agricultural field sizes (from 0.5 to 20 ha) produced by the economic model ProLand on hydrological processes using the IOSWAT model in the German Aar watershed. These authors emphasize the importance of using a comprehensive groundwater representation compared to a simple linear storage approach in areas characterized by a complex hydrological regime with an underlying aquifer system. Thanapakpawin et al. (2006) applied a distributed hydrology soil vegetation model (DHSVM) to the Mae Chaem River basin, in Thailand, to simulate forest-to-crop expansion and crop-to-forest reversal scenarios based on land-cover transitions observed from 1989 to 2000. The calibration and validation carried out revealed that the preferential flows were not reasonably captured by the simple linear reservoir routing mechanism used to represent the sub-surface flows.

Lin et al. (2007) linked a spatially explicit land-use change model (CLUE-s) and a combined distributed/lumped parameter hydrological model developed by Haith and Shoemaker (1987) to investigate the impact of land-use changes on the hydrology of the Wu-Tu watershed in Northern Taiwan. They conclude that combining a spatially explicit land-use simulation model with a hydrological model is an effective tool for investigating the impact of land-use change on hydrological processes, and promote the development of a landscape eco-hydrological decision-support system for watershed land-use planning,

management, and policy. In a subsequent study conducted in the same watershed, Chu et al. (2010) also used CLUE-s, but this time combined with a physically based distributed hydrological model (DHVSM). They conclude that the hydrological processes in a watershed are highly sensitive to the spatial distributed values of hydrological parameters and that therefore, it is important to use distributed hydrological models when investigating the impact of land-use composition and patterns on the hydrology of a watershed.

Hurkmans et al. (2009) applied a variable infiltration capacity (VIC), large-scale semi-distributed hydrological model to investigate the impact of land-use changes on stream flow generation within the Rhine basin in Western Europe. Land-use change scenarios were simulated up to 2030 using Dyna-CLUE (Verburg et al. 2006), a spatially explicit land-use change model, based on four emission scenarios defined by IPCC (2000). Their results indicate an increase in stream flow mainly due to urbanization. The authors found that the use of a physically based evapotranspiration module offers the advantage of minimizing the use of calibration parameters. However, the VIC model does not support bare soil evaporation, and the evapotranspiration was greatly underestimated specially during the winter period. These authors highlight the importance of using a physically based model that simulates all relevant hydrological processes.

Niehoff et al. (2002) generated land-use change scenarios using a spatially distributed land-use change modeling kit (LUCK). This was accomplished by increasing the percentage coverage of a single land use at a time and then investigating its impacts on hydrological processes using a process-oriented distributed hydrological model (WaSiM-ETH). These authors found that the combination of spatially distributed land-use scenarios and process-oriented hydrological models has great potential.

Oogathoo (2006) applied the physically based distributed hydrological model MIKE SHE to the Canagagigue Creek watershed in Ontario, Canada to evaluate the impact of management scenarios on the hydrological processes of the watershed by applying land-use increase/decrease percentages (e.g., increase urbanization from 0.2 to 2%). A comprehensive surface runoff (2-D diffusive wave approximation of the Saint Venant equations) and groundwater flow (3-D finite difference method) mechanisms were employed. The author emphasized the potential of MIKE SHE for investigating hydrological problems of diverse complexity and for simulating alternative management practices, particularly in Canadian contexts. A comprehensive evaluation of several well-known hydrological models conducted in Ontario, Canada, also confirmed MIKE SHE as being a comprehensive and flexible integrated model environment (AquaResource Inc 2011).

Xiang ([2004]) applied Precipitation Runoff Modeling System (PRMS), a semi-distributed and physically based model, and Streamflow Synthesis and Reservoir Regulation (SSARR), a lumped model, to investigate the impact of climate and urbanization change and logging on flood generation in the Elbow River watershed. The author found that the performance of the SSARR model was suited for the upper and lower basins during dry, medium, and wet climate conditions, while the performance of PRMS was only suited for the upper basin for only medium and wet climate conditions. The results revealed that the increased urbanization and logging have given rise to increased peak flows, volume, and earlier time to peak. The author also found out that PRMS did not perform well for river routing between the upper and lower river basins within the watershed.

In an initial study on the Elbow River watershed, Wijesekara et al. ([2012]) applied MIKE SHE/MIKE 11 linked with a land-use cellular automata (CA) model to investigate the impact of land-use change on hydrological processes for the period 2001–2031. The simplified linear reservoir method was used to represent the groundwater flow. An observation made during the calibration and validation of MIKE SHE is that this model underestimated the stream flow due to the inadequate production of baseflow from the saturated zone that could not be corrected by the linear reservoir method. The authors concluded that the use of a more comprehensive method to represent the groundwater flow in the saturated zone along with the physical sub-surface information was crucial for the Elbow River watershed in order to successfully represent the complex surface–groundwater interactions. It was also found out that a more comprehensive model setup (in terms of data and parameters) was required to improve the calibration of the model for the Elbow River watershed.

Objective

The objective of this paper is to describe a comprehensive land-use change/hydrological modeling system that was rigorously calibrated and validated for the Elbow River watershed and used to simulate four land-use change scenarios over a period of 20 years. This modeling system is designed as a spatial decision-support system for land-use planning and water resource management.

In this study, a CA model simulates dominant land-use changes in a spatially explicit context by considering historical trends and spatial/non-spatial constraints. This CA is linked to the hydrological model MIKE SHE/MIKE 11 where complex surface–groundwater interactions are modeled physically and in a distributed way. The coupling of these models allows us to accommodate the physical and distributed nature of the land-use changes and to successfully simulate the complex surface–groundwater interactions that exist in the watershed. The performance of the hydrological model was maximized through rigorous calibration and validation procedures that involve multiple time periods, climate conditions, and land-use allocations.

Compared to the initial study conducted by Wijesekara et al. ([2012]), the following improvements have been incorporated in the current setup.

Land-use change model:

- The historical maps used to calibrate the land-use CA model were revised to remove attribute errors due to imperfect geo-referencing.
- Additional constraints (forest reserves and planned clear-cut areas) were used during the simulation to better reflect the conditions existing in the watershed.

Hydrological model:

- A comprehensive 3D groundwater model was implemented to replace the linear reservoir method.
- Multiple criteria (calibration against stream flow and total snow storage, validation against groundwater levels) were applied, whereas calibration and validation were implemented only against stream flow in the previous study.
- Observations at one additional location (05BJ009) were considered for the stream flow comparison when evaluating the performance (goodness of fit) of the modeling system.
- Multiple validation periods (1991–1995, 1995–2000, 2000–2005, and 2005–2008) were used instead of only one (2000–2005) in the previous study.
- Additional data were used for the setup of the model (river branches, groundwater/surface water extractions, and river cross sections digitized from LiDAR).
- Additional land-use-based parameters were used (detention storage, paved runoff coefficient, and overland-groundwater leakage coefficient).
- Some of the datasets used in the initial study were replaced by data of higher accuracy (DEM, station-based precipitation, initial groundwater table, soil properties, and snow melt coefficient).
- Additional distributed parameter values were introduced (detention storage, paved runoff coefficient, overland-groundwater leakage coefficient, soil properties, and snow melting threshold).
- Finally, the modeling system was used to investigate the impact of four scenarios of land-use change on the hydrological processes of the watershed.
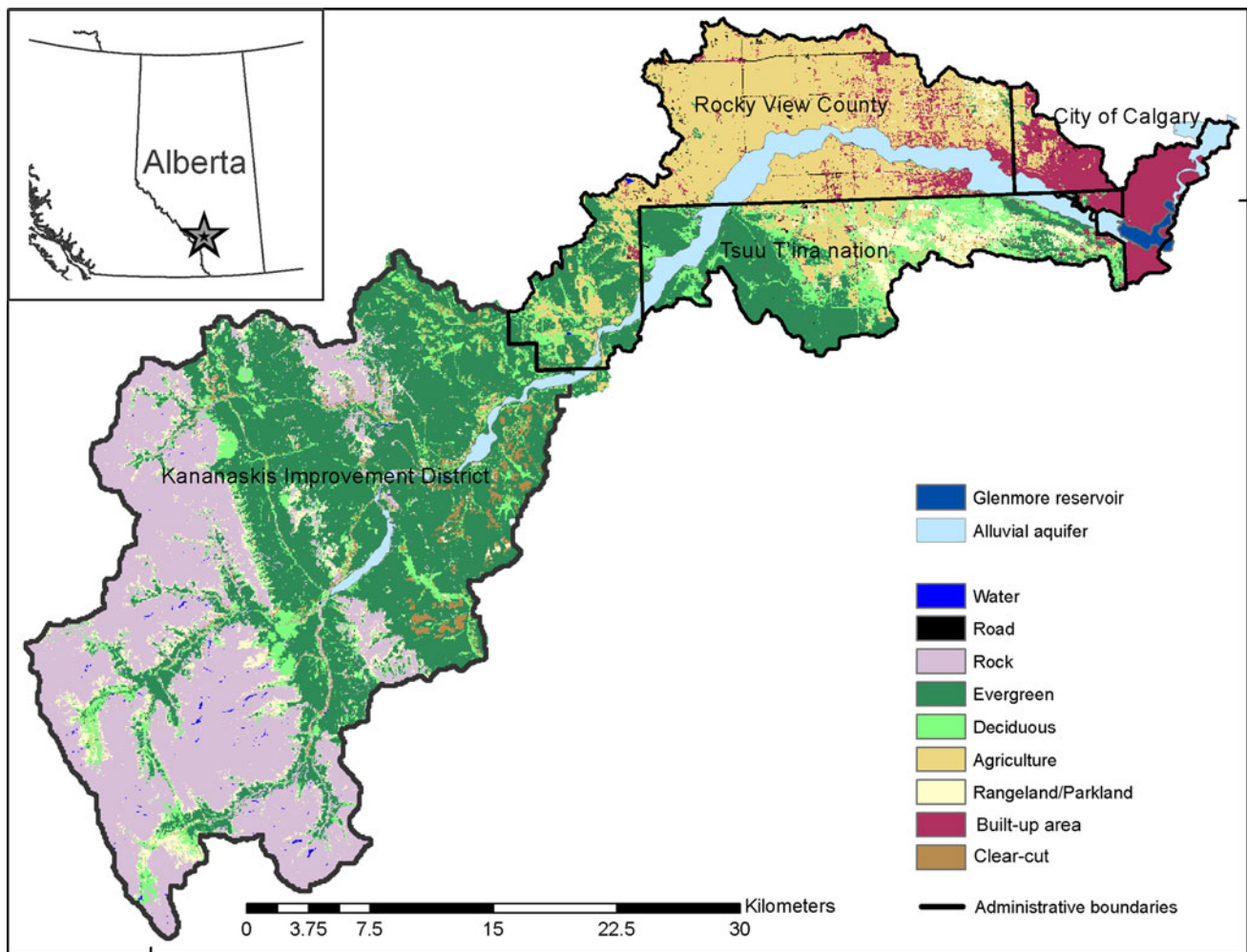
Fig. 1 Map of the Elbow River watershed

Methods

In this section, a description of the Elbow River watershed is first provided, followed by a presentation of the modeling framework and its components.

The Elbow River Watershed

The Elbow River watershed located in southern Alberta, Canada, drains an area of 1,238 km² through the Elbow River and its tributaries (Fig. 1). Sixty-five percent of the watershed is located in the Kananaskis Improvement District, while the remaining area is divided among the Rocky View County (20%), the Tsuu T'ina nation (10%), and Calgary (5%), a fast growing city of over one million inhabitants. The land-use composition within the watershed consists of urban area (5.9%), agriculture (16.7%), rangeland/parkland (6.2%), evergreen (34%), and deciduous forest (10%). Forest clear-cut areas can be observed in

about 1.8% of the watershed; the remainder of the watershed consists of rock, road, and water.

The Elbow River flows for approximately 120 km; it drops from 2,000 m elevation at Elbow Lake to 1,000 m where it enters the Bow River in downtown Calgary. Compared to other major rivers in the region, it is a short and steep river system where any impacts at the upstream due to land-use activities are readily transmitted downstream (Bow River Basin Council 2010; ERWP 2012). Furthermore, the watershed is characterized by a complex hydrological regime (Wijesekara et al. 2012; ERWP 2012) in which considerable surface—groundwater interaction exists between the river and the alluvial aquifer located in the north-east portion of the watershed (Fig. 1). The alluvial aquifer is a shallow unconfined aquifer representing 5% of the entire area of the watershed. It has been formed by alluvial deposition and is generally very permeable and highly hydraulically connected to the river, resulting in relatively fast groundwater flow through the shallow aquifer.
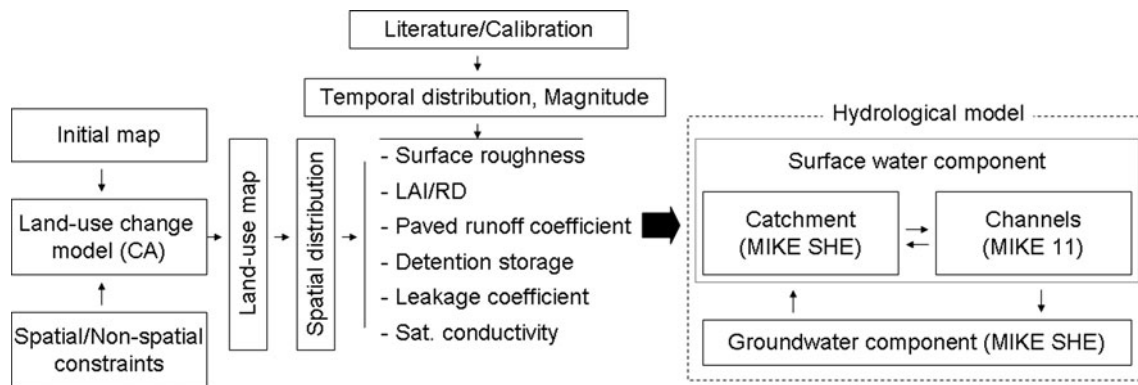
Fig. 2 The architecture of the coupled land-use-hydrology modeling system

In addition to representing an important source of water for irrigation, the Elbow River supplies approximately 40% of Calgary's drinking water through the Glenmore reservoir (Valeo et al. 2007). The water production for municipal use has almost reached its maximum capacity, and sustaining the future demands of the city of Calgary will be a challenging task. Moreover, lying in the rain shadow of the Rocky Mountains, this watershed is part of the Western Prairie Provinces (WPP), which is considered the largest dry area of southern Canada, where the average annual potential evapotranspiration is higher (800–900 mm) than the average annual precipitation (400–600 mm) (Coote and Gregorich 2000; Schindler and Donahue 2005, 2006).

The recent industrial development in Alberta and rapid increase in population affects the watershed, already under considerable pressure for land development in Bragg Creek, Redwood Meadows, and Rocky View County (Fig. 1). During the period 1985–2010, the civic census reveals a 71% population increase in Calgary (Schindler and Donahue 2006; The City of Calgary 2010). Forecasted population growth of the Calgary Economic region from 2011 to 2021 is estimated at 26% (Statistics Canada 2012; The City of Calgary 2012). The new land developments to the west of the city of Calgary combined with the ones occurring in the areas of Bragg Creek, Redwood Meadows, and the Rocky View County have the potential of evolving into several major and minor business corridors along the main highways (Rocky View County 2012) (Fig. 1). It is predicted that in the near future, rapidly increasing human activity will combine with climate warming, through its effect on glaciers, snow packs and evaporation, and cyclic droughts, to cause a crisis in water availability in this area (Schindler and Donahue 2006). To ensure water resource sustainability in the watershed, it is crucial to investigate the changes in land-use (historical and future) and their impact on the land phase of the hydrological cycle.

The Modeling Framework

The modeling framework includes three dynamic models that were linked: (1) a CA model developed in-house and applied to simulate land-use changes, (2) a hydrological model, MIKE SHE, set up with physically based, distributed surface and groundwater components to simulate the hydrological cycle, and (3) the MIKE 11 river model, a distributed detailed channel model to simulate the channel component as part of the surface water (Fig. 2). A hydrological conceptual model was designed for the Elbow River to guide the selection of appropriate data and methods and to simplify the model configuration based on acceptable assumptions for the particular focus of the study (Refsgaard 1997).

Based on an initial map representing the land-use patterns in a given year, the CA model simulates land-use changes, taking into account the influence of the neighborhood along with external spatial and non-spatial constraints. The spatial distribution of the land-use-based parameters (e.g., surface roughness) generated at each year of the simulation is then inputted into MIKE SHE/MIKE 11.

The following sections provide a description of the land-use CA model ("The Elbow River Watershed" section), the configuration ("The modeling Framework" section), calibration and validation of the MIKE SHE/MIKE 11 setup ("The Land-Use CA Model" section), the linkage between the land-use CA and MIKE SHE/MIKE 11 through the land-use-based parameters, and the four land-use change scenarios that were simulated using the modeling system ("The Hydrological Model" section).

The Land-Use CA Model

CA models are remarkably effective at simulating spatial land-use patterns and structures of the landscape. Unlike

traditional land-use change models, they are spatially explicit, highly adaptable, and relatively simple, while being able to capture a wide variety of dynamic spatial processes. A CA is a dynamic simulation model that represents space as a grid of regular cells with each cell being assigned an attribute that denotes its state, (e.g., land use). A local or extended neighborhood delineated around each cell is used to capture the influence on the central cell. The state of each cell evolves through discrete time steps based on transition rules that take into account the values of the cells within its neighborhood and some additional constraints that can be incorporated in the model (White and Engelen 2000). CA are widely used for the simulation of land-use/land-cover changes (Barredo et al. 2003; Li et al. 2003; Stevens et al. 2007; Ménard and Marceau 2007; Almeida et al. 2008; Shen et al. 2009; Santé et al. 2010; Wang and Marceau 2013).

The CA model has been developed in-house and applied in previous studies to investigate the land-use dynamics in the Elbow River watershed (Hasbani et al. 2011; Wijesekara et al. 2012; Marceau et al. 2013b). Historical land-use maps produced from Landsat Thematic Mapper imagery acquired during the summers of 1985, 1992, 1996, 2001, 2006, and 2010 at the spatial resolution of 30 m were used for calibration and validation as explained in details below. These maps contain nine dominant classes: water, rock, roads, agriculture, deciduous, evergreen, rangeland/parkland, urban areas, and forest clear-cuts. The quality of these maps was assessed through field verification and the use of third-party maps (from Google). They were further revised to ensure their temporal consistencies using an in-house computer program designed to detect and correct minor spatial-temporal inconsistencies in the historical maps due to classification and georeference errors (Wijesekara 2013).

In order to select the best configuration of the CA model for the study area, a sensitivity analysis was carried out to evaluate the influence of the cell size, neighborhood configuration, and external driving factors on the simulation results. The details of this analysis can be found in Hasbani et al. (2011). It revealed that a cell size of 60 m, a neighborhood configuration consisting of three concentric rings (distance from the center: 300, 540, and 1,020 m), and four driving factors (distance to the Calgary city center, distance to a main road, distance to a main river, and the ground slope) were the most appropriate to capture the land-use changes in the watershed. This model setup, including the four driving factors, was then used to derive the transition rules for the calibration of the CA model.

During the calibration, eight land-use state transitions corresponding to the changes identified in the historical land-use maps were considered (Table 1). The calibration procedure is a semi-automatic approach, meaning that it is conducted through a graphical user interface (GUI)

Table 1 Land-use transitions considered during the simulations

From	To
Evergreen	Agriculture
	Built-up area
Deciduous	Agriculture
	Built-up area
Agriculture	Rangeland/parkland
	Built-up area
Rangeland/Parkland	Agriculture
	Built-up area

where the modeler is engaged. For each land-use transition that is under consideration, the cells that have changed state in the historical maps are identified along with the number of cells of a particular state in their neighborhood and the values of each driving factor. This provides information about the particular conditions that prevailed around each cell that has historically changed state. This information is displayed through the interface in the form of frequency histograms (for example, number of cells that have changed state from agriculture to built-up area when being at certain distances from a main road). These histograms are then used by the modeler to identify the most prominent groups of values that will become the parameter values of the transition rules (Hasbani et al. 2011). A sensitivity analysis revealed that this grouping should be concentrated around the mode to obtain the parameters that generate the best simulation outcomes. These values are stored in a table and further used to determine the conditional transition rules of the model, which take the form of:

> If distance to a main road is between 100 and 800 m and number of built-up cells within the first neighborhood ring is between 0 and 15 and distance to downtown Calgary is between 1,000 and 2,300 m then the central cell might change from Agriculture to Built-up area.

All possible transition rules are created by combining the identified ranges of values from the frequency histograms (Hasbani et al. 2011).

The advantage of these conditional transition rules is that they have an inherent geographic meaning and are easy to interpret by the modeler. They are automatically converted by the model into mathematical rules. This allows the use of a quantitative index, referred to as the resemblance index (RI) to determine if a cell will change state or not. The RI is based on the Minimum Distance to Class Mean algorithm commonly used in remote sensing (Richards 2006). The mathematical rules are built by calculating the mean and standard deviation of the defined ranges of

values on the frequency histograms, which become the coefficients of the parameters of the transition rules. Using the coefficients of each transition rule, the resemblance index is calculated using Eq. 1, which quantitatively describes the similarity between the conditions prevailing in the neighborhood of a cell at the time step of the simulation, and the conditions observed in the neighborhood, which have been used to generate the values of the parameters of the transition rule.

$$\text{RI} = \sum_{i=1}^{m} \frac{|n_i - \bar{x}_i|}{\sigma_i} \qquad (1)$$

where m is the number of layers (corresponding to the number of external driving factors plus the number of land-use classes multiplied by the number of neighborhood rings), n_i is the value in layer i, $\bar{x}_i$ is the mean value for layer i in the transition rule, and σ_i is the standard deviation for layer i in the transition rule. If the standard deviation is zero for layer i, then $\frac{|n_i - \bar{x}_i|}{\sigma_i} = 0$ if $n_i = \bar{x}_i$ or otherwise equals positive infinity. Accordingly, $\text{RI} \in \Re^+$ and the smaller RI is, the more similar are the conditions surrounding a cell to the ones used to define the transition rule; this cell is, therefore, likely to change state (Hasbani et al. 2011).

In all simulations, two local constraints were applied to respectively forbid new built-up development within the Tsuu T'ina Nation reserve and to restrict any changes in the forest reserves within the Kananaskis Improvement District. The calibration of the CA model was conducted using the historical maps of 1985 to 2001 to simulate land-use changes up to the years 2006 and 2010. The maps of 2006 and 2010 that were not used for calibration were employed for validation by comparing them to the simulated land-use maps of the same years. The comparison was undertaken using a neighborhood of five cells to capture the land-use patterns while dismissing the exact spatial location within the neighborhood (Hasbani 2008). A percentage of correspondence was calculated by dividing the correct number of cells in all land-use categories by the total number of cells within the neighborhood and by taking an average of the calculated percentages for the entire map. A correspondence of 96 and 91% was obtained for the years 2006 and 2010, respectively. Based on these results, the CA model was considered sufficiently well calibrated for the purpose of this study. To project land-use change in the future, the CA model was re-calibrated using all the existing historical maps (1985–2010) to capture the most recent land-use dynamics that occurred in the watershed in the transition rules.

The Hydrological Model

The MIKE SHE flow model integrated with the MIKE 11 river model is capable of simulating all major processes in the land phase of the hydrological cycle (Graham and Butts 2005; Sahoo et al. 2006; Refsgaard et al. 2010). These processes include snowmelt, evapotranspiration (ET), overland flow, unsaturated flow, and groundwater flow. For each of these processes, MIKE SHE offers several configuration approaches that range from simple, lumped, and conceptual, to advanced, distributed, and physically based.

MIKE SHE was dynamically linked to the one-dimensional hydrodynamic surface water model MIKE 11 for a complete representation of the river network within the watershed. The configuration includes comprehensive surface water and groundwater components (Fig. 3), which are described in detail below. It tightly couples several modules representing different hydrological processes and their exchange flows (DHI 2009). A detailed description of the relevant data and parameters used in the MIKE SHE/MIKE 11 setup, including climate data, topography, vegetation parameters, land-use-based hydrological parameters, channel flow data, and the initial groundwater table is provided in Table 6 (Appendix).
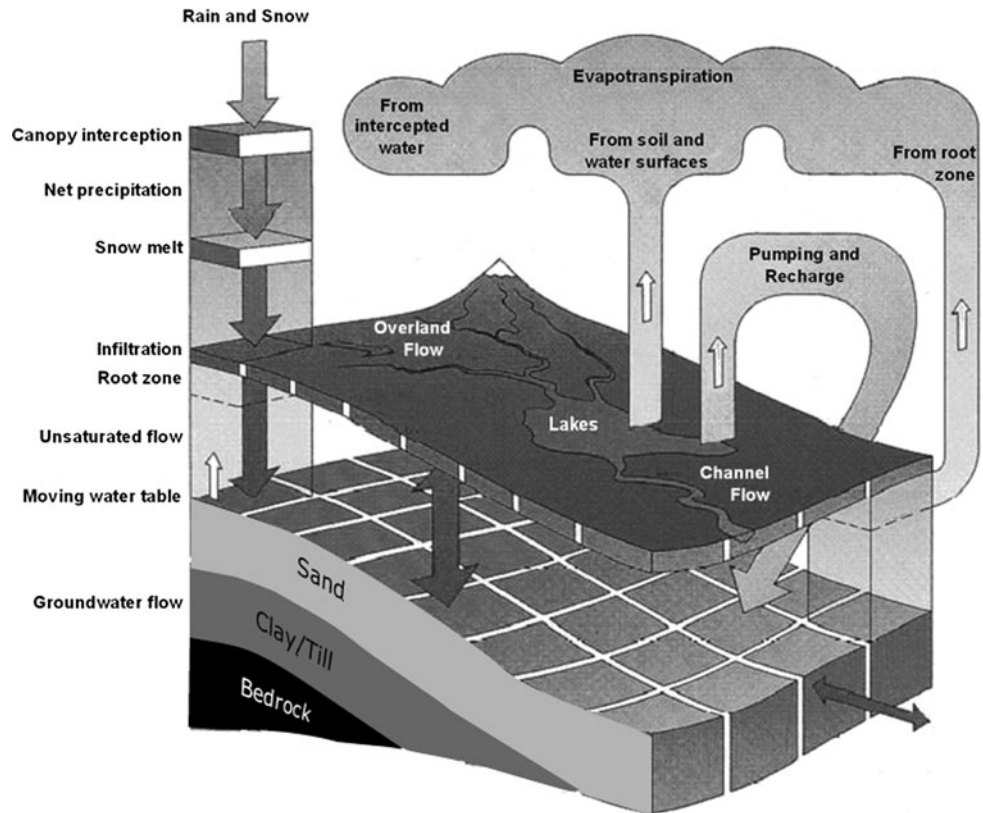
Surface Water Component

The surface water component includes the overland flow and channel flow processes that are represented by comprehensive methods. Each grid element representing the watershed contains a unique set of physical properties that governs the changes of the overland flow, which was simulated using a finite difference method within MIKE SHE. This method solves a two-dimensional diffusive wave approximation of the Saint Venant equations to calculate the surface flow in the x- and y-directions and the water depths for each grid cell of the model domain. The relevant equations can be found in Wijesekara et al. (2012).

Channel flow is represented by the fully dynamic solution of Saint Venant equations to simulate surface water along the river channels in order to accurately calculate the exchange flow between the channels and the overland flow. The governing equations used in this method are the vertically integrated equations of conservation of continuity and momentum. More details can be found in Wijesekara et al. (2012).

The associated data and parameters required for simulating the overland flow are topography, surface roughness, detention storage, and overland-groundwater leakage coefficient; the ones employed for setting up the MIKE 11 channel flow module include digitized river network with tributaries, cross sections, surface water extractions, boundary conditions, and river bed resistance. They are described in Table 6 in Appendix. MIKE SHE and MIKE 11 were integrated using the links created with each river reach/branch in MIKE 11 with the surface water components of MIKE SHE.

Groundwater Component

A groundwater model based on a 3D finite difference method was adopted to represent the saturated zone of the Elbow River watershed. This approach uses sub-surface layer information including hydro-geologic stratification and hydro-geologic properties for each layer. The 3D finite difference algorithm calculates flow by describing mathematically the spatial and temporal variations of the dependent variable (hydraulic head) using a 3-dimensional Darcy equation solved numerically by an iterative implicit finite difference technique. The saturated zone component of flow interacts with the other components in MIKE SHE primarily by using flow terms from the other components implicitly or explicitly as source or sink terms.

Three geological layers (sand, clay/till, and bedrock) were used to represent the saturated zone (Fig. 3). Twenty-four new geological parameters were created for these layers, i.e., vertical and horizontal hydraulic conductivity, specific yield, and specific storage for six geological units (alluvial aquifer, sand and gravel, clay/till, bedrock, top layer of the mountains, and clay/river) used to define the three layers. The spatial distribution of these geological units within each geological layer as configured within the MIKE SHE/MIKE 11 setup is illustrated in Fig. 14 in Appendix. The final values of each geological parameter

after calibration are listed in Table 2. To consider the water extraction from the bedrock aquifers within the 3D groundwater module, a total of 145 licensed groundwater pumping wells was included; it was assumed that 50% of the water extracted from these wells will return to the groundwater following its use. Details about the initial groundwater table used in the simulation of the groundwater component are provided in Table 6 in Appendix.

In addition to the surface and groundwater components, the snow melting process within the watershed was simulated with the snowmelt module of MIKE SHE, which uses the modified degree-day method (Leaf and Brink 1973). Between surface water and groundwater, the flow within the unsaturated zone was assumed vertical and was modeled using the two-layer water balance method (Yan and Smith 1994) in the current setup of MIKE SHE/MIKE 11. The scientific background of each of these methods can be found in Wijesekara et al. (2012).

Calibration and Validation of the Hydrological Model

The flow chart of actions taken to carry out the calibration and validation of the hydrological model is illustrated in Fig. 4. A number of calibration parameters (listed below and described in Table 6 in Appendix) were selected to run the sensitivity analysis prior to the calibration and

Table 2 Values of geological parameters in saturated zone after calibration

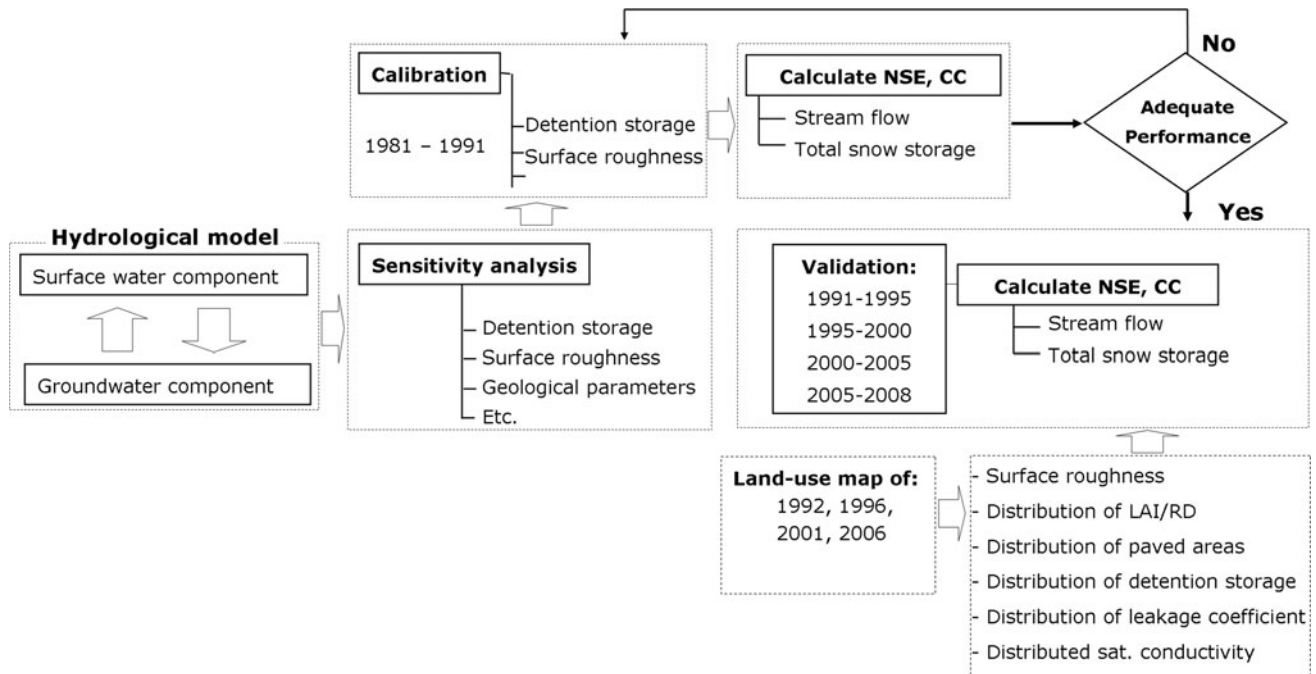| Geological unit	Soil code (SZ)	Horizontal conductivity (m/s)	Vertical conductivity (m/s)	Specific yield (−)	Specific storage
Alluvial aquifer	1	0.0004	4e−005	0.2	0.001
Sand and gravel	2	1e−005	2e−006	0.2	0.001
Clay/till	3	1e−008	1e−009	0.05	0.0005
Bedrock	4	5e−008	5e−009	0.05	0.0005
TopLayer_Mt (Top Layer on the mountains)	5	0.0005	0.0002	0.1	0.001
Clay/river	6	1e−006	1e−007	0.2	0.001

Fig. 4 Calibration and validation procedure for the hydrological model

validation. Physical data (listed and described in Table in 6 Appendix) were used when available in all the physically based methods (e.g., surface roughness in the finite difference method to simulate overland flow). This procedure greatly minimized the number of calibration parameters within the hydrological model. First, the sensitivity of the model to various parameters (detention storage, snowmelt parameters, riverbed leakage coefficient, riverbed resistance, and geological parameters associated with the geological layers) was analyzed. The sensitivity analysis to surface water parameters was conducted by manually changing the values of each parameter at a time and running simulation from 1981 to 1991. With each run, the goodness of fit of the model was evaluated by comparing observed and simulated total snow storage and stream flow data (details are provided later in this chapter). This was repeated by changing the values of the parameters in combination (changing values of more than one parameter at a time). This approach was implemented intuitively since the number of combinations of parameter values can be large.

Secondly, a sensitivity analysis was carried out for all 24 geological parameters of the 3D groundwater module; stream flow data (generated baseflow contribution) were used to evaluate the sensitivity of the model. This analysis was done by: (i) changing the value of a single parameter for each geological unit at a time, (ii) changing two or more (maximum 4) parameters for each geological unit at a time, (iii) changing the value of a single parameter in more than one geological unit at a time, and (iv) changing multiple parameters in multiple geological units at a time, in a sequence. The remaining geological parameters at each stage were kept constant. Since testing every combination was practically unattainable, about 150 different combinations were selected intuitively.

The sensitivity analysis to surface water parameters revealed that snow melt affected the total snow storage, while the other parameters affected the stream flow. This further indicated that the simulation of stream flow was mostly sensitive to detention storage, and the simulation of total snow storage to all snowmelt parameters. The sensitivity analysis to geological parameters revealed that mainly the vertical and horizontal hydraulic conductivity parameters of the 3D groundwater model had an impact on the stream flow generation (as a result of changing baseflow and infiltration) and the temporal changing pattern of the generated groundwater table (with the change of infiltration). Based on this outcome, initial values were assigned to each hydrological component, and the values of the most sensitive parameters were further refined during the calibration. When adjusting the values for horizontal and vertical hydraulic conductivity, the fact that the horizontal conductivity is typically 5–10 times higher than the vertical hydraulic conductivity was considered.

Based on the results obtained from the sensitivity analysis, a rigorous calibration and validation procedure was applied to the hydrological model based on different methods as recommended by Refsgaard (1997), i.e., split-sample, multi-criteria, and multi-point. The split-sample method emphasizes the use of different time periods for the calibration and the validation and a different land-use map as input for each validation. The multi-criteria method emphasizes the use of different criteria to evaluate the goodness of fit of the model based on different categories of observed data (i.e., use of stream flow and groundwater level to evaluate the overall goodness of fit). The multi-point method emphasizes the use of observed data from different spatial locations for the evaluation of the goodness of fit for the calibration and the validation (i.e., use observed data at points A and B for calibration, and observed data at points C and D for validation).

The model grid size was set to 200 m due to the high computational time required for the model to complete simulations at finer spatial resolutions. The calibration was based on the time period 1981–1991 using the land-use map of 1985. The quality of the calibration was measured using goodness-of-fit coefficients calculated on the total snow storage and stream flow. Observations from several stations were used to implement a rigorous calibration: measurements of snow storage at one snow station (Little Elbow) and measurements of stream flow at four hydrometric stations (05BJ009, 05BJ006, 05BJ004, 05BJ010) (Fig. 5). In addition to snow storage and stream flow, observed groundwater levels at 20 locations were available. Groundwater levels at these locations were simulated for comparison with observed groundwater levels during calibration.

The validation was carried out based on four different time periods (1991–1995, 1995–2000, 2000–2005, and 2005–2008) using the land-use maps relevant to each validation period, i.e., 1992 land-use map for 1991–1995, 1996 land-use map for 1995–2000, 2001 land-use map for 2000–2005, and 2006 land-use map for 2005–2008. The goodness of fit was calculated by comparing observed and simulated data using the Nash and Sutcliffe coefficient of efficiency (NSE) for stream flow and the Pearson's correlation coefficient (CC) for total snow storage. Additionally, the mean absolute error (MAE) was also calculated for the comparison of observed and simulated groundwater levels. Many other indices were calculated to evaluate the goodness of fit of the MIKE SHE/MIKE 11 model setup against simulated stream flow, such as Ln NSE, relative NSE, and coefficient of determination for more rigorous stream flow comparison; details can be found in Wijesekara (2013). Only the results based on NSE and CC are indicated in this paper for simplicity.

Evaluating the Impact of Land-Use Changes on Hydrological Processes

Evaluating the impact of land-use changes on hydrological processes involves four main steps: (i) providing the initial land-use map and relevant spatial/non-spatial constraints to simulate future land-use changes, (ii) setting relevant land-use-based parameters and deriving their spatial distribution from each forecasted land-use map, (iii) configuring the hydrological model based on changed land-use-based parameters to run simulations, and (iv) extracting information related to each hydrological component which is then compared and analyzed considering the different land-use changes.

A total of four scenarios of land-use changes were simulated with the CA model: the business as usual scenario (BAU) based on the assumption that future land-use changes will be similar to past observed changes, a scenario with a new centralized development plan (RV-LUC) based on a potential growth point identified by Rocky View County (2012), a scenario with a new centralized development in the area of Bragg Creek (BC-LUC), and a scenario where land-use is changed based on the forecasted population trends according to the City of Calgary (2012) (P-LUC). For all scenarios, the simulations were carried out with the land-use CA model for the years 2016, 2021, 2026, and 2031 using the initial land-use map of 2010. Using forest harvest sequence data obtained from Alberta Environment Sustainable Resource Development (AESRD), clear-cut areas associated with each future year (2016, 2021, 2026, and 2031) were overlaid on each simulated land-use map to take into account the possible changes in the forested portions of the watershed.

These simulated land-use maps were used to provide the spatial distribution of the land-use-based parameters needed for MIKE SHE/MIKE 11. Assigning corresponding values
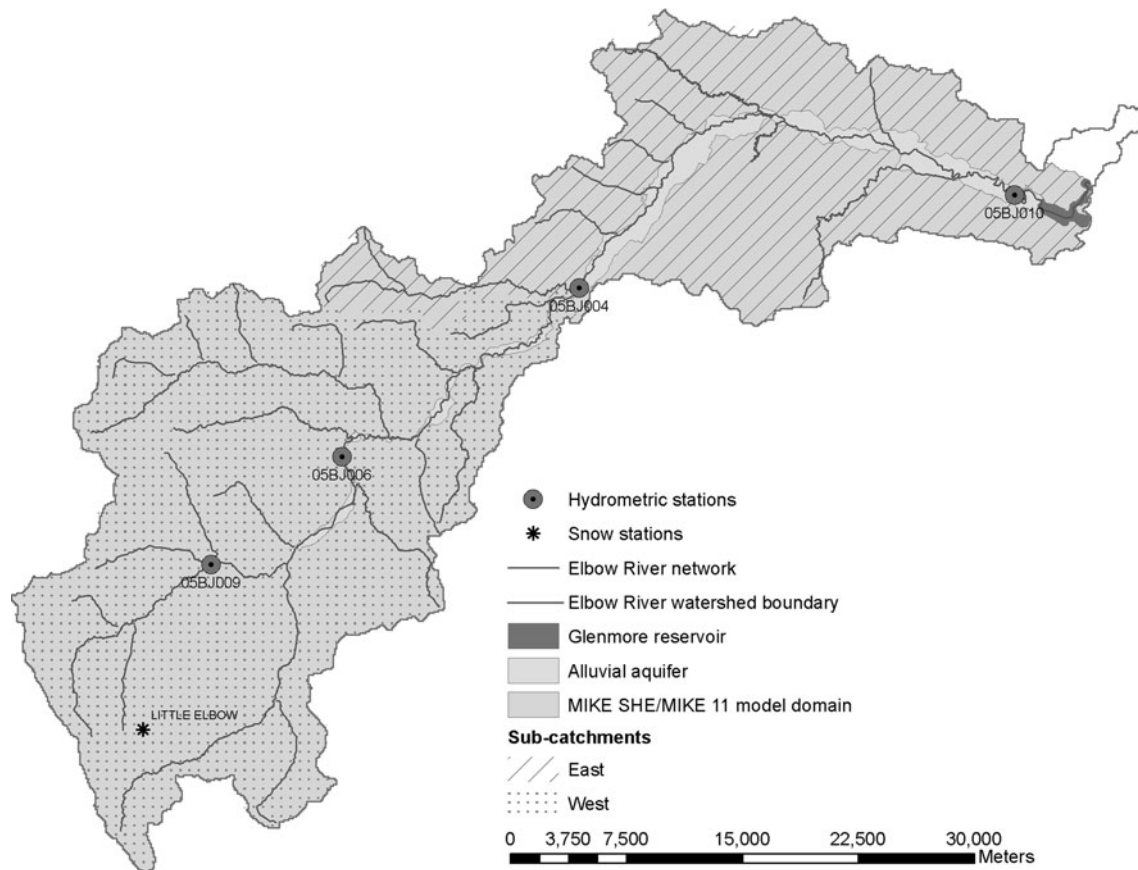
Fig. 5 Location of the hydrometric stations, snow stations, and groundwater level stations in the east and west sub-catchments used for the calibration and validation of the hydrological model

to each land-use class, spatially distributed maps of surface roughness (Manning's M) were created for each land-use map. Areas of urban development were overlaid onto the soil maps to define paved areas; these areas within the soil distribution maps were assigned a low saturated hydraulic conductivity value of 2.7e-012 m/s. The spatial distribution of vegetation properties (LAI and RD) was changed according to the distribution of the corresponding land-use class in each land-use map. Furthermore, for each land use, a distributed value for detention storage, paved runoff coefficient, and overland-groundwater leakage coefficient were created as indicated in Table 6 in Appendix.

To evaluate the impact of land-use changes on the hydrological processes, simulations were conducted for a period of five years using the land-use-based parameters and their spatial distribution based on the historical land-use maps of 1992, 1996, 2001, 2006, 2010, and simulated land-use maps of 2016, 2021, 2026, and 2031. The non-land-use-based data (i.e., river channel, topography, geological layers, etc.) and other parameters (i.e., snow melt parameters, ET surface depth, etc.) were kept unchanged. The climate data (daily precipitation, reference ET, daily

temperature) used for these simulations were the same as the data employed within the validation period (2000–2005). The initial value of snow storage was set to 0 mm as each simulation was started on the 1st of September (beginning of the fall season). The initial conditions for sub-surface potential heads were derived from the previous simulation (1995–2005).

The simulations were carried out with the output frequency of channel flow set at 24 h and at 72 h for overland flow, snow melt, ET, and unsaturated zone flow. After each simulation, using the MIKE SHE water balance tool, the total water balance error, total overland flow (OL), total evapotranspiration (ET), total infiltration (Inf), and baseflow (BF) for the entire catchment within the 5 year simulation period were obtained and tabulated for the east and west sub-catchments of the watershed separately (Fig. 5).

Results and Discussion

The results of the calibration and validation of the hydrological model against total snow storage and stream flow

are presented in Tables 3 and 4, respectively. An average correlation coefficient of 0.86 was achieved for the calibration against total snow storage, while it is 0.80 for the validation (Table 3). This calibration, which has not been undertaken in the initial study of Wijesekara et al. (2012), indicates a good performance of the model in calculating the snow storage in colder climate conditions. An average NSE value of 0.63 was achieved for both the calibration and validation using daily observed and simulated stream flow data, while it is 0.74 using monthly observed and simulated data (Table 4). These results represent an improvement of -0.02 and 0.5, when using the daily and monthly data, respectively, compared to the previous study of Wijesekara et al. (2012). In comparison, Oogathoo (2006) obtained an average performance with NSE values of 0.59 and 0.40 for the calibration and validation of MIKE SHE, respectively, when applied to the Canagagigue Creek watershed in Ontario.

According to the hydrological model guidelines of Moriasi et al. (2007), this indicates good model performance in generating stream flow by the surface water processes (e.g., overland flow) and groundwater processes (e.g., baseflow). While daily and monthly NSE values calculated for the station 05BJ009 are low (0.2), the correlation coefficient obtained for this station reaches 0.68 and 0.84 for daily and monthly values, respectively (table not shown due to space constraints). The calibration and validation results based on other indices (Ln NSE, relative NSE, and coefficient of determination) against simulated

and observed stream flow also revealed a good performance of the model (Wijesekara 2013). The WB error (%) in each simulation period (Table 4) represents the total water balance error (mm) as a percentage of the total precipitation (mm) (WB error/Total precipitation × 100) during the corresponding simulation period. This error is considered minimal when it is less than 1% (Oogathoo 2006).

When evaluating the quality of the calibration and validation against simulated and observed groundwater levels, it was noted that for calculating comparison indicators (CC, MAE), too few observed points were available relative to the simulated values in each station. For example, a maximum of nine observed values were available for a station, whereas simulated values were generated at every 2–4 hours (depending on the model time step in each iteration) during a simulation period of five years. Furthermore, the observed groundwater level data presented quality issues. For example, in some stations, the groundwater levels were found higher than the observed ground surface elevations. Typically, the calibration of a hydrological model against groundwater levels is required in order to find the appropriate values for the geological parameters and to obtain a good performance in simulating the groundwater levels. A well-calibrated groundwater model also sufficiently produces baseflow to surface streams. In our model, the goodness of fit of the hydrological model against stream flow was found to be sensitive to the parameter values of the geological layers. Therefore, in order to determine the best fitting values for the geological parameters, the contribution of baseflow in the total stream flow was recognized as a better indicator than the simulated groundwater levels.

Figure 6 shows selected graphs (amongst 19 different graphs) illustrating the comparison between the observed and simulated stream flow at station 05BJ004 and station 05BJ010, and total snow storage at the Little Elbow station. These graphs show a very good visual correlation between the observed and simulated stream flow and total snow storage at the corresponding stations. Overall, the above results indicate a high performance of the model and were

Table 3 Results of the calibration/validation of the hydrological model based on total snow storage

	Calibration/Validation period	Correlation coefficient Little Elbow
Calibration	Sept. 1981 to Dec. 1991	0.86
Validation	Sept. 1991 to Dec. 1995	0.77
	Sept. 1995 to Dec. 2000	0.70
	Sept. 2000 to Dec. 2005	0.84
	Sept. 2005 to Dec. 2008	0.86

Table 4 Results of the calibration/validation of the hydrological model based on stream flow (009, 006, 004, and 010 are corresponding to the hydrometric stations, 05BJ009, 05BJ006, 05BJ004, and 05BJ010, respectively, from upstream to downstream)

|	Calibration/validation period	WB error (%)	NSE—daily				NSE—monthly			
			009	006	004	010	009	006	004	010
Calibration	Sept. 1981 to Dec. 1991	0.04	0.53	0.63	0.72	0.63	0.63	0.75	0.83	0.75
Validation	Sept. 1991 to Dec. 1995	0.06	0.25	0.63	0.75	0.75	0.23	0.69	0.90	0.86
	Sept. 1995 to Dec. 2000	0.08	N/A	N/A	0.77	0.64	N/A	N/A	0.87	0.79
	Sept. 2000 to Dec. 2005	0.05	N/A	N/A	0.72	0.64	N/A	N/A	0.83	0.82
	Sept. 2005 to Dec. 2008	0.04	N/A	N/A	0.53	0.6	N/A	N/A	0.69	0.77
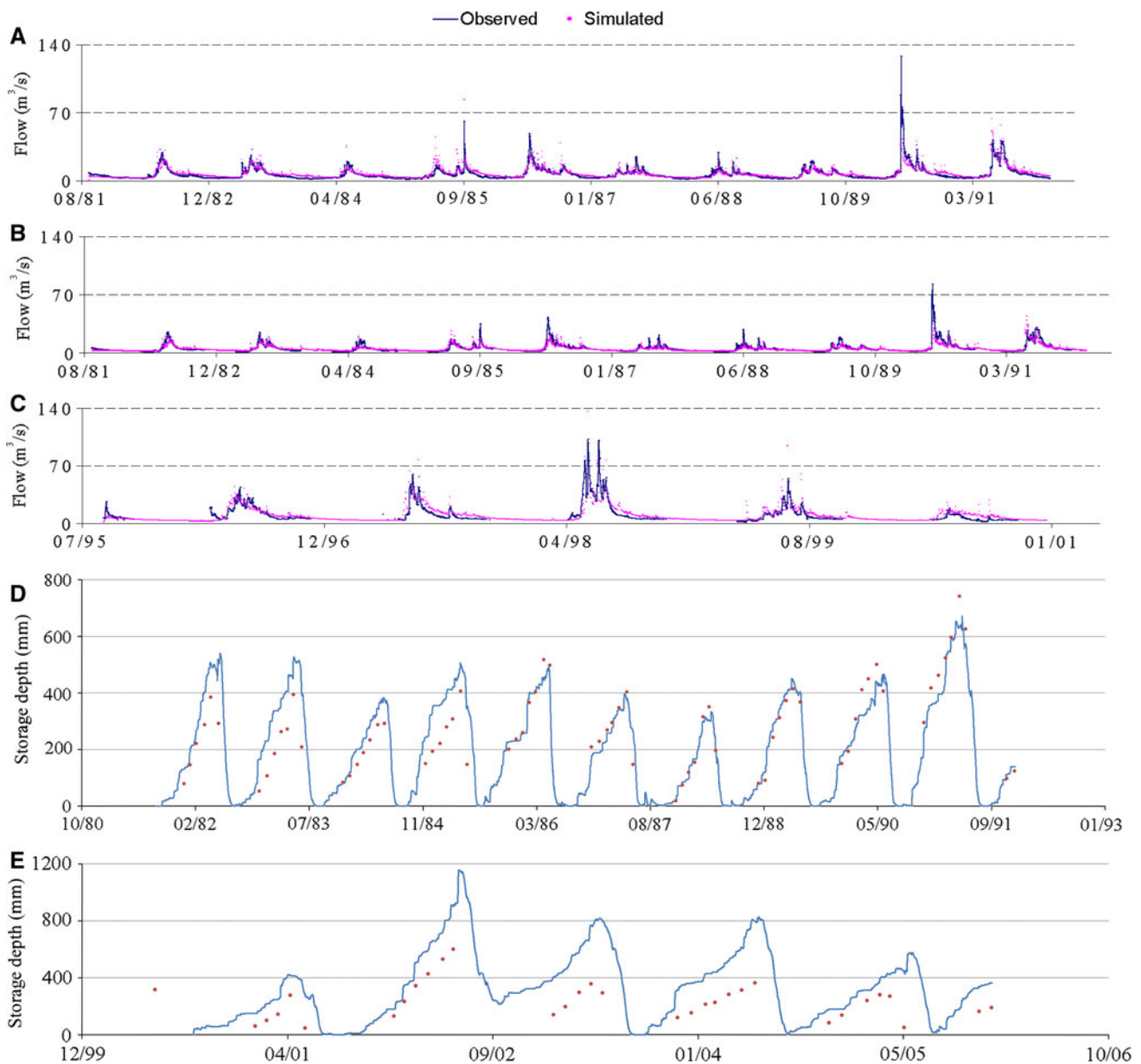
Fig. 6 Observed and simulated stream flow at station 05BJ004 during 1981–1991 (**a**), 05BJ006 during 1981–1991 (**b**), 05BJ010 during 1995–2000 (**b**), and total snow storage data at station Little Elbow during 1981–1991 (**c**), and 2000–2005 (**d**)

found adequate to evaluate the impact of scenarios of land-use changes on hydrological processes.

Impact of Land-Use Changes on Hydrological Processes for the Period 1992–2010

Since different land-use changes dominate in the east and west sub-catchments of the watershed, they are described separately in this section. The east sub-catchment is dominated by built-up areas and agriculture. Due to the considerable growth of built-up areas (117%) over the period 1992–2010, the evergreen and deciduous forest areas have been reduced by about 8 and 11%, respectively, along with agricultural areas (9%) (Fig. 7a). Areas of rangeland/parkland have increased by 3%. In comparison, the west sub-catchment is dominated by evergreen and deciduous forests. From 1992 to 2010, evergreen forest was reduced by 8%, while the reduction reaches 28% for the deciduous forests (Fig. 7b). Clear-cuts were minimal in 1992, but started increasing in the year 2000 to reach a peak value in 2010 (2.7% of the west sub-catchment). The reduced forest areas have been replaced by clear-cuts and rangeland/parkland.

Figure 8(1) shows the variation of each hydrological process in storage depth (mm) (accumulated flow within
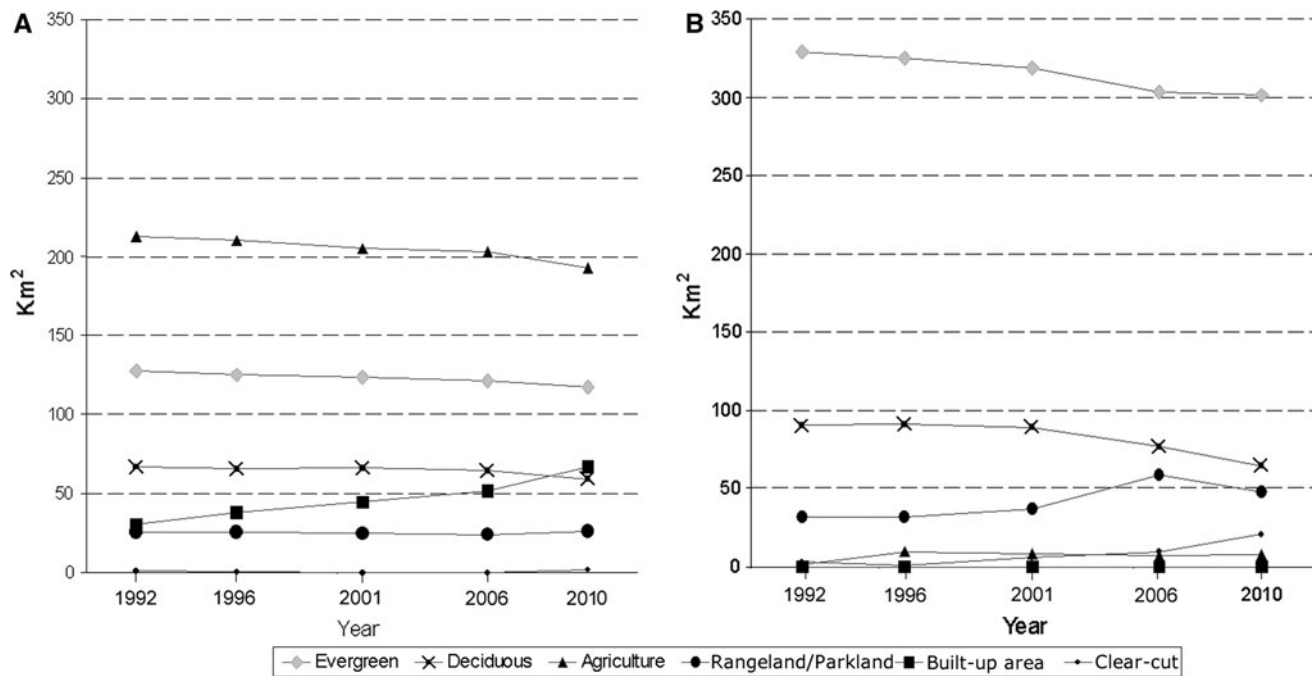
Fig. 7 Land-use change for the period 1992–2010 in the east sub-catchment (**a**) and the west sub-catchment (**b**)

the simulation period of five years) against land-use change within the east and west sub-catchments over the period of 1992–2010 (hydrological model run with land-use maps of 1992, 1996, 2001, 2006, and 2010). Figure 8(2) shows the percentage increase or decrease of the hydrological processes for the east and west sub-catchment over the period 1992–2010. Within the east sub-catchment, the dominant variations are an increase of 121% in overland flow, and a decrease of 1.7% in baseflow, 3.5% in evapotranspiration ,and 15% in infiltration. These variations are explained by the increased urbanization over the years and the reduction of forested areas.

Forest and rangeland/parkland areas in the west sub-catchment produce relatively less overland flow, providing more opportunity for water to infiltrate (Manning's M is 33.33 indicating high surface resistance) compared to built-up areas (Manning's M is 90.9 indicating very low surface resistance). Furthermore, the detention storage is about 20 mm for both forest and rangeland/parkland areas resulting in more infiltration and evapotranspiration compared to built-up areas where the detention storage is almost null. Consequently, these vegetated areas generate low overland flow with higher infiltration, evapotranspiration, and baseflow. In the east sub-catchment on the other hand, built-up areas create more overland flow with less infiltration, evapotranspiration, and baseflow. Therefore, compared to the variations of hydrological processes that can be observed in the east sub-catchment, the variations in the west sub-catchment are minimal (Fig. 8b).

Impact of Land-Use Change Scenarios on the Hydrological Processes for the Period 2016–2031

Since the dominant land-use changes occur within the east sub-catchment of the Elbow River watershed, the following results are presented for that sub-catchment only. Figure 9(1) illustrates the simulated land-use changes for four scenarios, while Fig. 9(2) shows the percentage increase or decrease of area for each land-use class corresponding to these scenarios. This percentage is the same for the scenarios BAU, RV-LUC, and BC-LUC and is, therefore, presented in a single graph in Fig. 9(1a). The growth of built-up areas reaches 25% with a corresponding reduction of agriculture (1%), evergreen (2.6%), and deciduous (19%) areas. For the scenario P-LUC (Fig. 9(1b), 9(2)), there is a substantial growth of built-up areas between 2016 and 2031 (46%), while the areas of agriculture, evergreen, and deciduous decrease by 5%, 4%, and 19%, respectively. The higher percentage increase for built-up areas reflects the projected population growth represented in that scenario.

Despite the fact that the scenarios BAU, RV-LUC, and BC-LUC have generated the same percentage increase/ decrease in area of land-use change, they have created different spatial patterns due to the varying spatial constraints applied during the simulations. As an example, these spatial patterns are displayed for the year 2031 in Fig. 10. In the BAU scenario, new built-up areas are
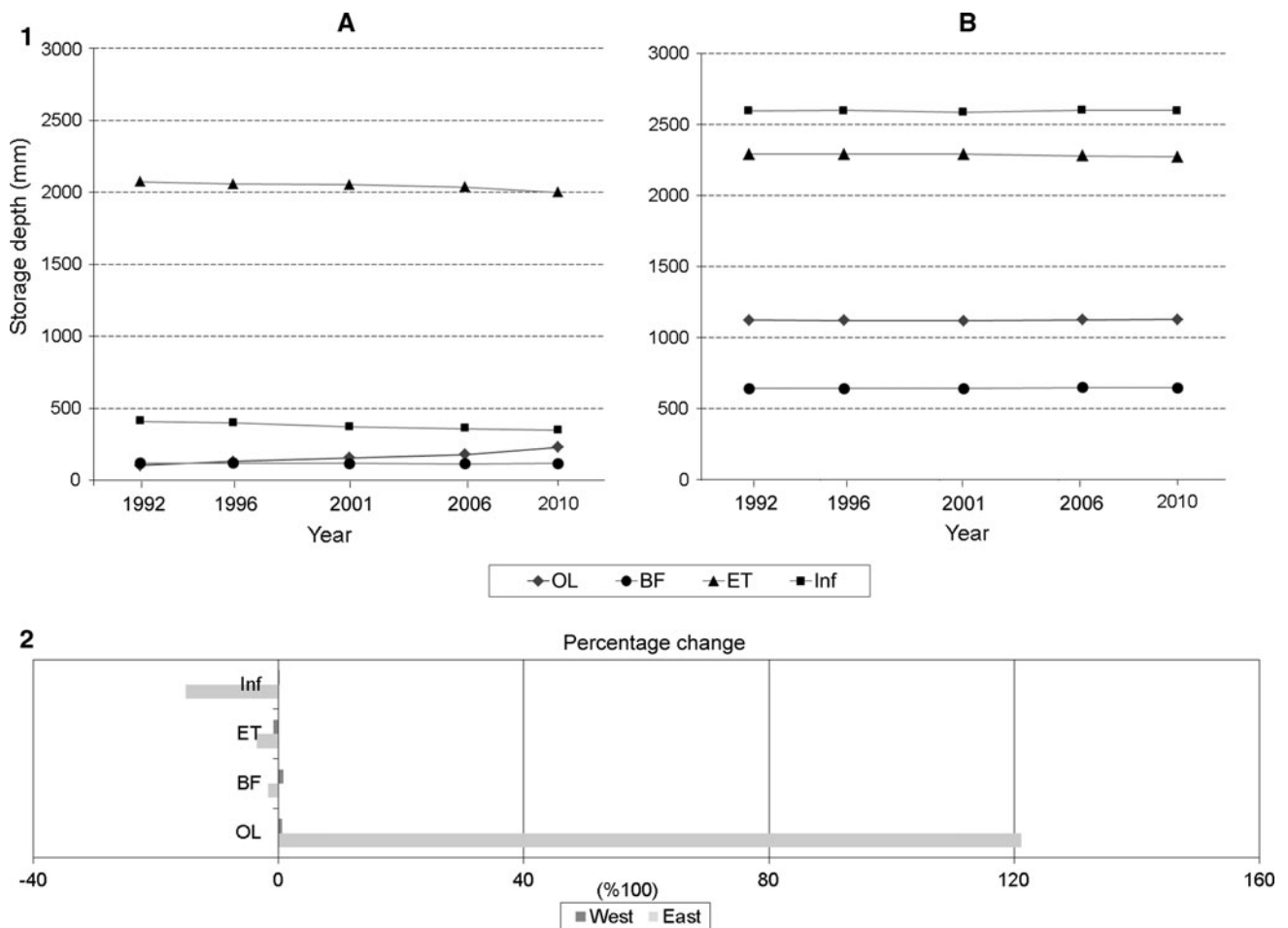
Fig. 8 (1) Variation of OL (overland flow), BF (baseflow), ET (evapotranspiration), and Inf (infiltration) for the east sub-catchment (**a**) and the west sub-catchment (**b**) for the period 1992–2010; (2) Percentage change between 1992 and 2010 in the east and west sub-catchment for each hydrological process

sparsely distributed to the west of Calgary compared to the scenarios RV-LUC and BC-LUC, where concentrated built-up areas appear within the Rocky View County and in the area of Bragg Creek, respectively. The scenario P-LUC generates more built-up areas appearing further west of the city of Calgary and in the north part of the watershed than the other scenarios. The spatial distribution of built-up areas in this scenario (P-LUC) is the same as for the scenario BAU.

The particular spatial patterns generated from the land-use maps affect the distribution of the land-use-based parameters (e.g., surface roughness). The non-land-use-based data and parameters (e.g., slope of the terrain) interact with these land-use-based parameters in a complex way to influence the hydrological processes. Figure 11 shows the impact of the land-use changes on each hydrological process for the period 2016–2031 within the east sub-catchment of the watershed. The scenario P-LUC generated the highest overland flow (average of 306 mm),

while the scenario RV-LUC generated the lowest overland flow (average of 273 mm) (Fig. 11a). This scenario has also produced the lowest baseflow (avg: 117 mm), evapotranspiration (avg: 1,922 mm), and infiltration (avg: 346 mm), while the RV-LUC scenario has produced the highest baseflow (avg: 118 mm), and infiltration (avg: 362 mm) (Fig. 11b, c, and d).

Although the scenarios BAU, RV-LUC, and BC-LUC generate the same amount of land-use changes over the years, their influence on the hydrological processes is different due to the particular land-use spatial distribution. For example, the average value of OL is the highest for BAU, is high for BC-LUC and is the lowest for the RV-LUC scenario (Fig 11a). The scenarios with similar patterns (P-LUC and BAU) also show a different impact on the hydrological processes. This is due to more built-up areas appearing in scenario P-LUC compared to the BAU scenario. Furthermore, the scenarios with the same type of constraints and the same percentage increase/decrease in
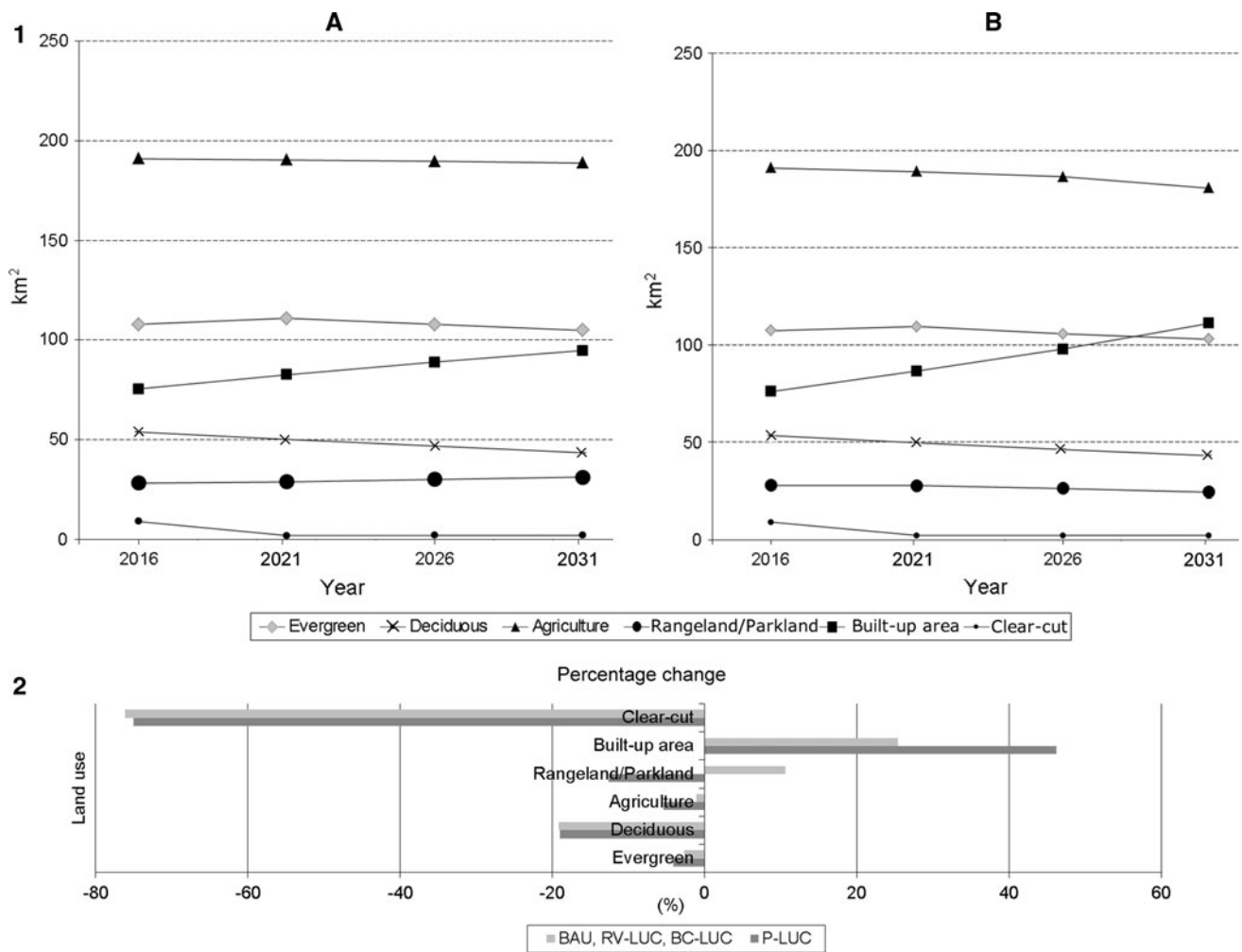
Fig. 9 (1) Simulated land-use changes during the period 2016–2031 in the east sub-catchment of the watershed based on Scenarios BAU, RV-LUC, BC-LUC (**a**) and Scenario P-LUC (**b**). (2) Percentage change between 2016 and 2031 for the BAU, RV-LUC, BC-LUC scenarios and P-LUC scenario for each land use

area (RV-LUC and BC-LUC) also generate different impacts on the hydrological processes, e.g., OL (Fig. 11a), mainly due to their particular location of concentrated development. This clearly illustrates that the amount of land-use change, its spatial distribution, and the location of a land development all affect the hydrological processes.

Figure 12 shows the percentage increase or decrease for each hydrological process over time for the four scenarios. The highest percentage increase in OL over the years occurs with the scenario P-LUC (40 %), while the other scenarios have generated an increase of between 23 and 25%. Furthermore, the highest percentage decrease of ET and Inf is produced with the scenario P-LUC, while the highest percentage decrease of BF occurs with the scenarios BAU, RV-LUC and P-LUC. The lowest percentage decrease of BF, ET, and Inf happens with the scenarios BC-LUC, BAU and RV-LUC, respectively.

More overland flow means that the water is not retained on the surface for infiltration and evaporation but drains away through the channels. This is caused by an increase in land uses such as built-up areas, which have a relatively low detention storage, surface roughness, leakage coefficient, and saturated hydraulic conductivity, and a high paved runoff coefficient. Less infiltration produces less groundwater recharge, which results in low contribution to the rivers through baseflow during the dry season. Therefore, the sustainability of the water in the rivers is affected. When the percentage change in the hydrological processes due to land-use change is high, the total accumulated impact over a long period can be considerably high in magnitude. For example, in our study, the scenario P-LUC can drain out more water over the years than the scenario BAU (Figs. 11, 12) resulting in less groundwater storage and baseflow.

Fig. 10 Predicted land-use maps for the year 2031 in the east sub-catchment of the Elbow River watershed according to the scenarios BAU (**a**), RV-LUC (**b**), BC-LUC (**c**), and P-LUC (**d**). For clarity, only built-up areas are displayed
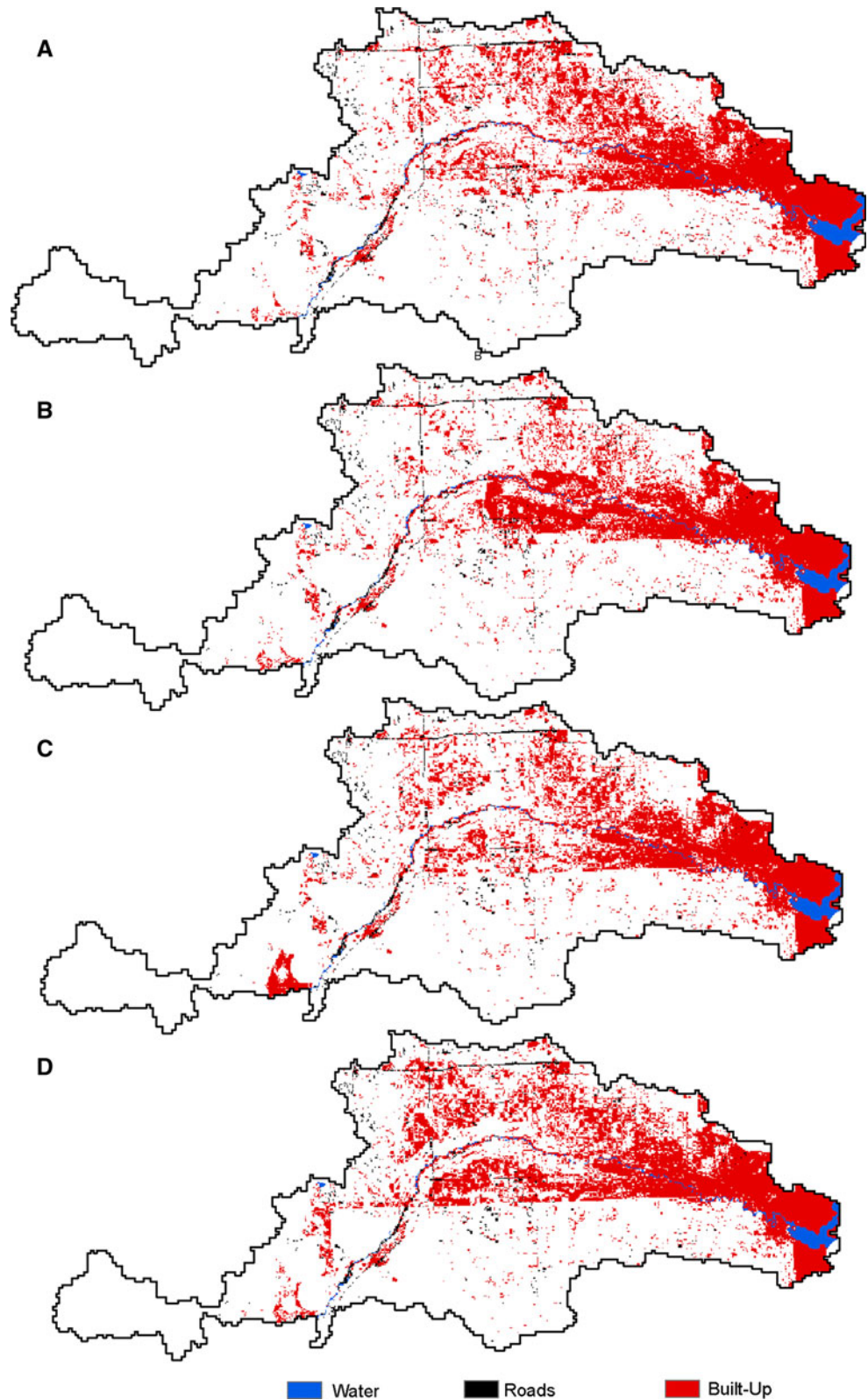
A decrease in the vegetative cover due to deforestation or land-use conversion into built-up areas (causing less transpiration and evaporation) results in a relatively low ET. Evapotranspiration is known to be the main driving force in landscape sustainability and to be instrumental in temperature and water distribution in time and space.
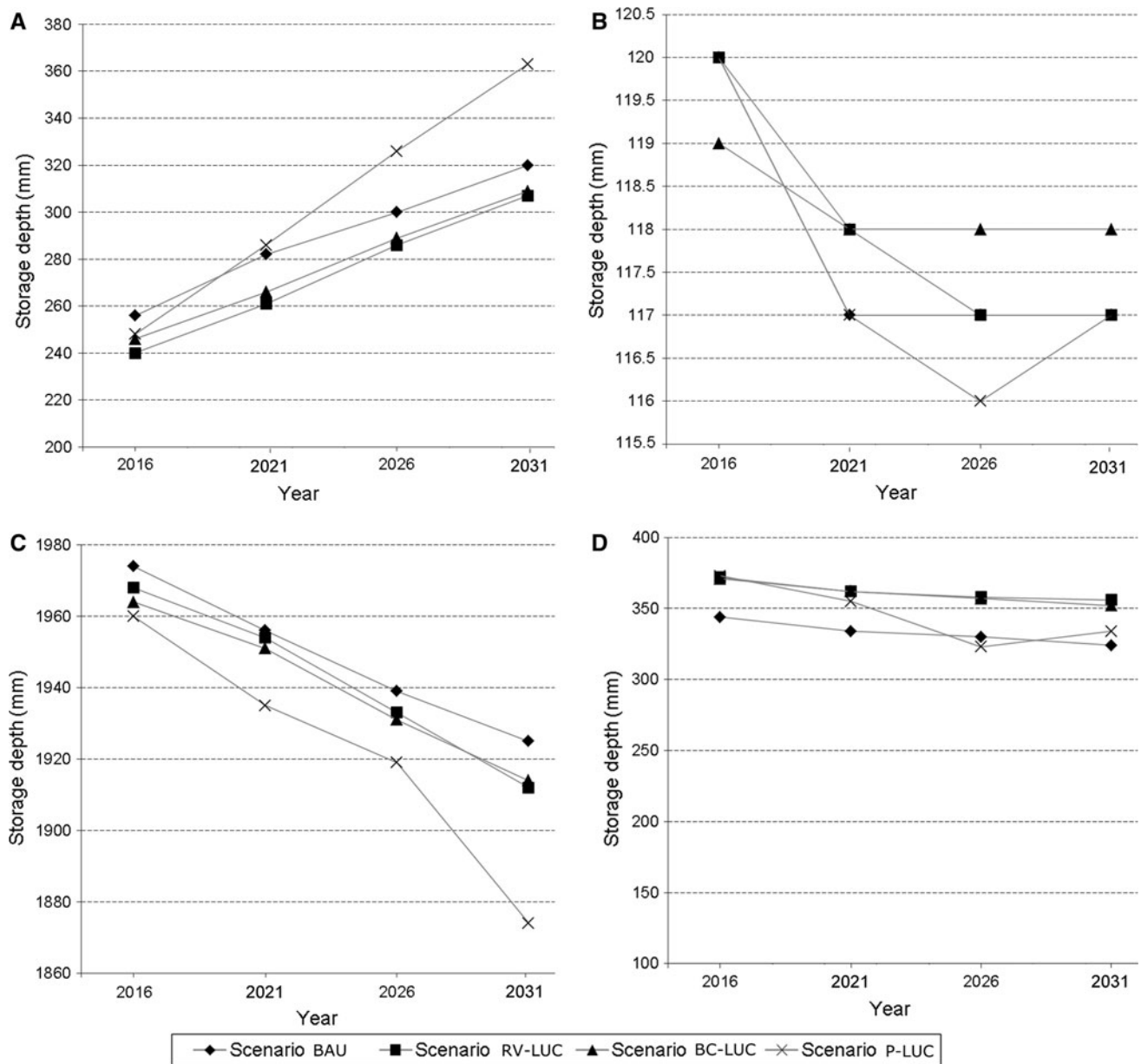
Fig. 11 Variation of OL (overland flow) (**a**), BF (baseflow) (**b**), ET (evapotranspiration) (**c**), and Inf (infiltration) (**d**) over time as a result of land-use change scenarios BAU, RV-LUC, BC-LUC, and P-LUC in the east sub-catchment during the period 2016–2031

Adequate evapotranspiration is crucial to keep the balance of the hydrological cycle, dissipate/re-distribute solar heat energy, and reduce the loss of organic matter that enriches the soil (Eiseltová et al. 2012). Therefore, a reduction in ET as a result of land-use change can produce more adverse effect to the environment and is undesirable.

This information was used to compare the four simulated land-use scenarios in terms of their "preferability." A scenario that comparatively generates low overland flow and high infiltration, baseflow, and evapotranspiration over time is considered as more "preferred." In contrast, a scenario that produces high overland flow and low

infiltration, baseflow, and evapotranspiration is considered as less "preferred."

Table 5 shows the total impact of each land-use change scenario on each hydrological process in 2031. The scenarios RV-LUC and BC-LUC are more preferable when considering overland flow. In terms of baseflow, the four scenarios are comparable with a slightly higher contribution to streams from BC-LUC. The scenario BAU is "preferred" considering its highest contribution to the atmosphere through evapotranspiration, while the scenario RV-LUC is "preferred" because of its highest contribution to the groundwater through infiltration. From being the

Fig. 12 Increase/decrease percentage of each hydrological process according to the land-use change scenarios: BAU, RV-LUC, BC-LUC, and P-LUC during the period 2016–2031 within the east sub-catchment (*OL* overland flow, *BF* baseflow, *ET* evapotranspiration, *Inf* infiltration)
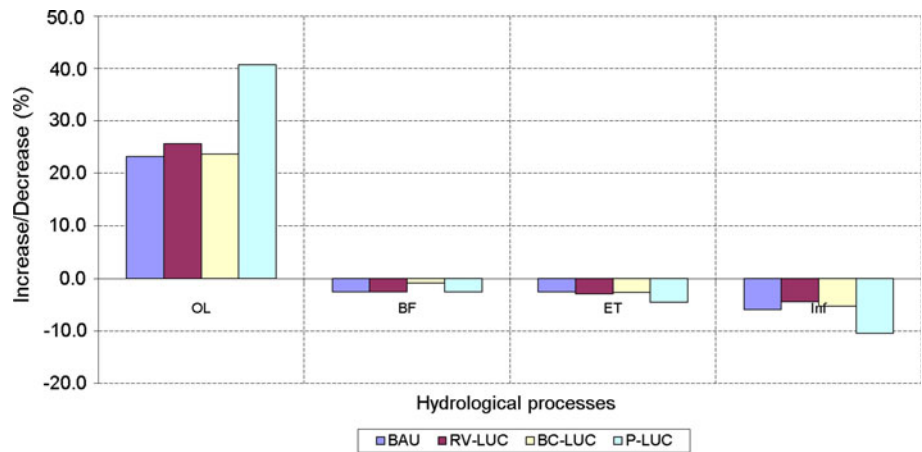
Table 5 Impact of each land-use change scenario on each hydrological process in 2031

Scenario	OL (mm)	BF (mm)	ET (mm)	Inf (mm)
BAU	320	117	*1,925*	324
RV-LUC	*307*	117	1,912	*356*
BC-LUC	309	*118*	1,914	352
P-LUC	363	117	1,874	334

The italicized values are the most preferred values for each hydrological process

most "preferred" to the least "preferred," the scenarios are ranked as follow: RV-LUC, BC-LUC, BAU, and P-LUC.

Changes in land-use also affect stream flow as illustrated for the period of May to December 2005, based on the simulated land-use map of 2031 (Fig. 13). An interesting observation is that the variation in stream flow is negligible over most of the period considered, except at particular moments in time corresponding to peak flows where the influence of the land-use scenarios becomes obvious. The two highest peak flows occurred on June 8 and 18, 2005 for which a warning was issued by Alberta Environment. Our simulations indicate that some land-use scenarios intensify these peak flows, which might lead to flooding. While the RV-LUC was selected as the most preferable scenario based on the values displayed in Table 5, this same scenario produced the highest river flows, most likely to cause flooding in the month of June of that year.

This figure highlights an important limitation of using changes in only storage depth for identifying preferred land-use change scenarios, namely that this approach does not consider the spatial distribution of changes in river
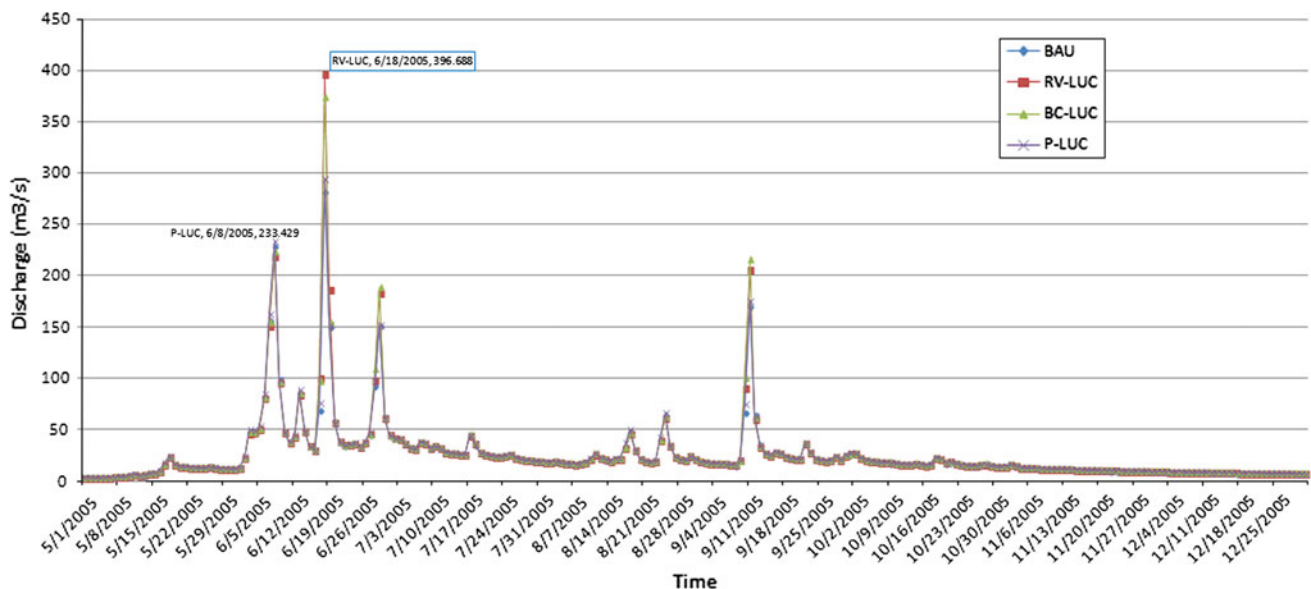

Fig. 13 Variation in discharge measured at the hydrometric station 05BJ010 corresponding to the four land-use change scenarios simulated for the year 2031

discharge, especially peak flow responses to land-use changes. These results underline the importance of considering multiple components of the hydrology of a watershed and their interrelations when assessing the impact of land-use changes. In order to produce meaningful conclusions, the analysis of river discharge, especially peak flow responses to land-use changes must be done comprehensively, which was outside the scope of our study. However, it would be possible to conduct such a systematic investigation with our modeling system in the future.

Conclusion

This paper describes the coupling of a spatially explicit land-use change model (cellular automata) with a distributed, physically based hydrological model (MIKE SHE/ MIKE 11) to study the impact of four land-use change scenarios on hydrological processes in the Elbow River watershed in Alberta, Canada. MIKE SHE and MIKE 11 models were configured to simulate the complex surface–groundwater interactions existing in the watershed. After rigorous calibration and validation, a Nash and Sutcliffe coefficient of efficiency (NSE) of 0.74 was obtained during both calibration and validation against observed and simulated monthly stream flow data. An average correlation coefficient of 0.86 and 0.80 was respectively achieved for the calibration and validation against total snow storage.

The analysis of the historical impact of land-use changes on the hydrological processes within the east sub-catchment characterized by considerable growth in built-up areas reveals an increase of runoff and reduced baseflow, infiltration, and evapotranspiration. The west sub-catchment is dominated by forest and rangeland/ parkland areas that have a higher water retention capacity compared to built-up areas; therefore, the impact of the land-use changes on the hydrological processes was found minimal.

The four scenarios of land-use changes that were simulated for the future (2016–2031) include: the business as usual scenario (BAU), a scenario with a new centralized development plan (RV-LUC) based on a potential growth point identified by Rocky View County (2012), a scenario with a new centralized development in the area of Bragg Creek (BC-LUC), and a scenario where land-use is changed based on the forecasted population trends according to Calgary Economic Development (2010) (P-LUC). It was found that, particularly in the east sub-catchment, the hydrological processes vary with the percentage increase/ decrease in land-use area, the generated land-use spatial patterns, and the location of concentrated land development if any.

The "preferability" of the scenarios was evaluated based on the impact of land-use changes on each hydrological process. When the overland flow is relatively high, while infiltration, evapotranspiration and baseflow are relatively low, the corresponding land-use change scenario is considered less "preferred"; it is more "preferred" when the opposite is true. The scenarios RV-LUC and BC-LUC were considered the most "preferred," while P-LUC was considered the least "preferred." However, this selection must be nuanced when considering the variation in discharge corresponding to the four land-use change scenarios, which revealed that the RV-LUC scenario produced the highest peak flow, indicating a risk of flooding during the month of June. These results highlight the importance of considering the spatial distribution of changes in river discharge, particularly peak flows when evaluating the impact of land-use change scenarios on the hydrology of a watershed. While considered outside the scope of this study, a systematic evaluation of the impact of land-use change scenarios on river discharge and peak flow responses could be done with our modeling system in the future.

While this study is the first of this nature to be carried out in the Elbow River watershed, it also contains unique aspects in comparison to similar studies conducted in different regions of the world. The modeling system that was developed incorporates three comprehensive models that fully represent the land-use changes and hydrological processes of the watershed. The land-use change and hydrological models are connected through an exhaustive set of land-use-based parameters that are spatially distributed. The modeling system offers the flexibility for the user in altering the data, parameters, and model configuration so that a variety of water related sustainability issues can be investigated within the watershed with a minimal amount of modifications. As an example, it can serve as a tool to find the location of a land development plan that will contribute to water resource sustainability. It could be used to explore a variety of land-use change scenarios from urban expansion to deforestation. It could be employed to quantify the total stream flow at various spatial locations, or to assess the impact of removing/adding new water licenses on the surface water (volume of water generated through stream flow).

Some limitations remain in this study. First, the calibration and validation of the MIKE SHE/MIKE 11 model setup against observed groundwater levels (as a third criterion in addition to stream flow and total snow storage) could not be implemented due to pending issues of data quality and availability of groundwater level data. As a result, the model cannot currently be employed to investigate the impact of land-use changes on the groundwater table. Second, the finest model grid resolution that could be

reasonably considered within the model configuration is 200 m mainly due to computational intensity of the simulations, even though land-use changes were observed and simulated at 60 m. Within the hydrological model, the land-use maps were re-sampled to the model grid resolution (200 m) which creates a loss of land-use details. However, a sensitivity analysis revealed that these losses have almost no impact on the hydrological processes (Marceau et al. 2013a, oral presentation).

Work is currently in progress to incorporate five regional climate change scenarios in the modeling system presented here to evaluate the independent and combined impact of past and future land-use and climate change on hydrological processes and to assess the sustainability of water resources in the Elbow River watershed under these conditions.

Appendix

See Table 6 and Fig. 14.

Table 6 Data and parameters used for configuring the hydrological model

Data	Description of data gathering and processing
Climate data	Daily precipitation, temperature, and potential evapotranspiration available for 1961–2008 were acquired from the Agroclimatic Atlas of Alberta that includes climate data from over 1,200 stations in Alberta and from about 1,400 stations bordering Alberta and British Columbia, Saskatchewan, Yukon, Northwest Territories, Nunavut and the United States. These climate data have been interpolated for each township of Alberta by the Government of Alberta (2008). In setting up MIKE SHE, raw station-based precipitation data were used by developing Thiessen polygon "areas of influence" for each station. The temperature and potential evapotranspiration data remained township based (Wijesekara and Marceau 2012). Furthermore, orographic effect on precipitation and temperature was represented by temperature lapse rate of $-0.75°C/100$ m and precipitation lapse rate of 10%/100 m (DHI Water and Environment 2010)
Topography	An 80 m resolution DEM from GeoBase (GeoBase 2008), re-sampled at 200 m, was used. This DEM was furthermore revised by adding and combining the bathymetry data of the Glenmore Reservoir (DHI Water and Environment 2010)
LAI—leaf area index and Root depth	The leaf area index (LAI) and root depth (RD) define the vegetation properties of the model domain. These components govern the precipitation interception on leafs, and the evaporation and water transpiration through roots. Each land use on the historical land-use maps has these properties that vary through time. LAI values vary from 0 to 7. During the full leaf period, Evergreen and Deciduous have a value of 5, while agriculture has a value between 2 and 4 during the summer period. For seasonal vegetation, this value drops to 0.2 during the winter months. Root depth values are average depths of actual root zone of the vegetation. Forest areas are usually defined with a higher root depth which is considered a constant. Root depth values for agricultural areas begin at 0, peak when the crops are fully grown, and drop down to 0 when the crops are harvested. For the MIKE SHE setup, the values for LAI and RD were derived from the literature (DHI Water and Environment 2010; Scurlock et al. 2001). The derived LAI and RD values for Water, Road, Rock, Evergreen, and Built-up are constants (where some of them are set to 0), while the LAI and RD values for Deciduous, Agriculture, Rangeland/Parkland, and Clear-cuts vary at each year
Manning number M (inversion of standard manning's n)	Manning's M defines the surface roughness of the land surface and governs the surface runoff. These values are derived from the literature, while their spatial distribution is based on each land-use map (Wijesekara et al. 2012). The values of Manning's M assigned to each land-use were: Water: 25.04, Road: 76.9, Rock: 40.0, Evergreen: 10.0, Deciduous: 10.0, Agriculture: 28.57, Rangeland/parkland: 33.33, Built-up: 90.9, Clear-cut: 90.9
Detention storage	Detention storage represents the threshold storage depth at land surface in each cell that must be filled before overland flow is generated. This parameter was used when the DEM could not adequately represent the details of topographic depressions due to the coarse scale of the model grid. Detention storage was defined for each land-use class as follows: Water: 0 mm; Road: 5 mm; Rock: 10 mm; Evergreen: 20 mm; Deciduous: 20 mm; Agriculture: 20 mm; Rangeland/Parkland: 20 mm; Built-up: 0 mm; Clear-cut: 0 mm (values determined through calibration)

Table 6 continued

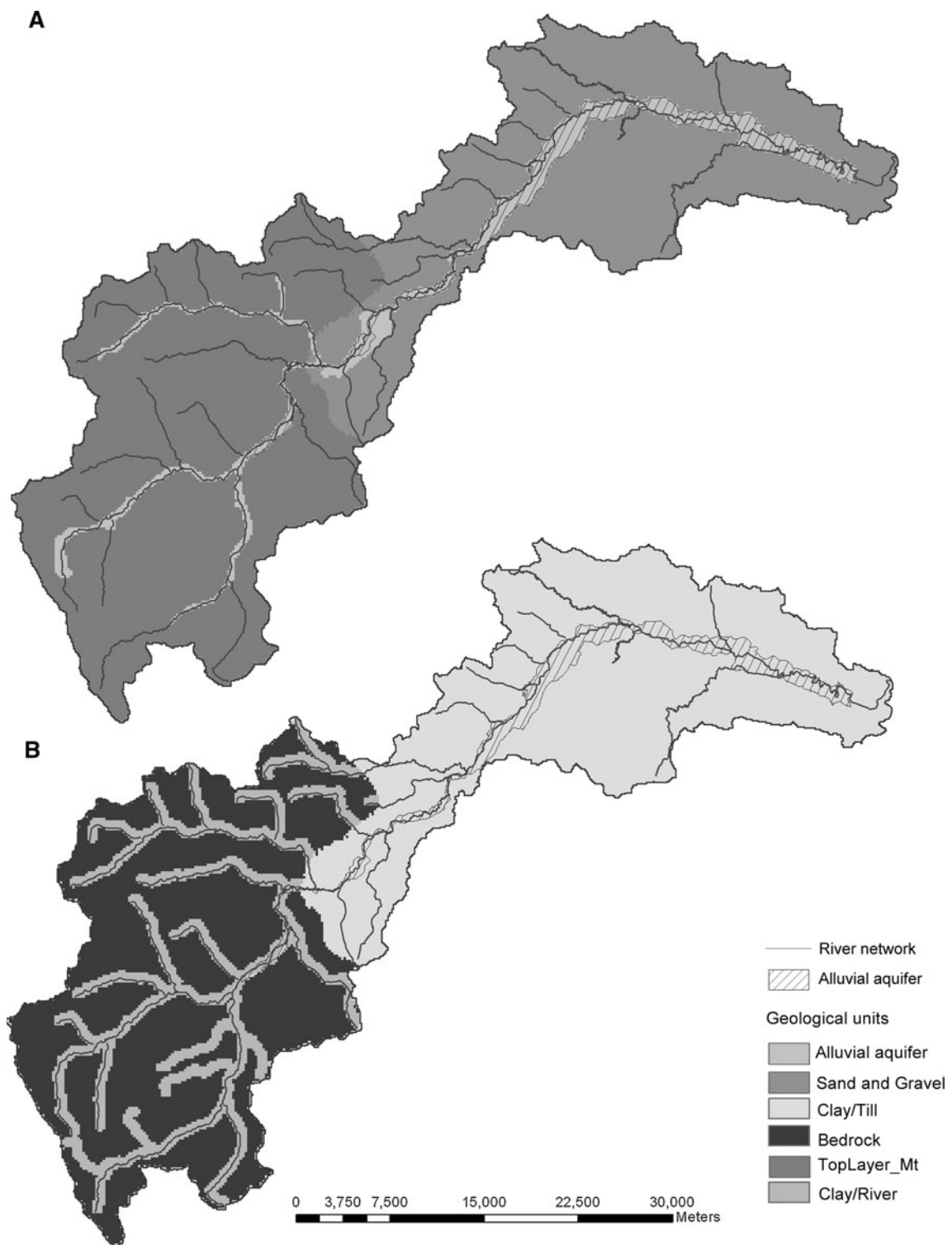| Data	Description of data gathering and processing
Paved runoff coefficient	This parameter determines the fraction of water from the overland flow that is directly transferred to the closest ponds/lakes/river links. A value of 1 (100% of overland flow is drained without any infiltration) was assigned to built-up areas
Overland-groundwater leakage coefficient	This parameter limits the infiltration rate and seepage outflow rate across the ground surface. A value of $1e-013$ m/s was assigned to built-up areas and the Glenmore reservoir (a minimum value was determined so that no infiltration will be produced)
Snowmelt parameters	Snowmelt can dramatically affect the spring runoff timing and volume. In MIKE SHE, it is determined by data and parameters such as air temperature, melting threshold temperature, degree-day coefficient, minimum snow storage, and maximum wet snow fraction. A temporal changing value for the degree-day coefficient parameter was derived using the information obtained from Kuusisto (1980) and was adjusted during calibration. A value of 0.5 °C for the melting threshold temperature in the mountainous area (elevation higher than 1,700 m) and a uniform value of 0 for the remaining area were used in ERWHM. These values were found during the calibration. Additional parameter adjustments done during calibration included setting the minimum snow storage value to 100 mm and the maximum wet snow fraction to 0.1 (DHI Water and Environment 2010)
Unsaturated zone flow and ET parameters	An 11-class soil classification map was included to represent the unsaturated zone. Appropriate soil parameters for each class were created and values were assigned to soil water content (at saturation, field capacity, and wilting point) and saturated hydraulic conductivity. MIKE SHE uses these parameters to determine the infiltration in the saturated zone. These parameters were calculated using average physical properties of different horizons in the UZ zone (data were obtained from Agricultural Region of Alberta Soil Inventory Database and the Canadian Soil Information Service Data sources). Furthermore, the soil maps were overlaid with the land-use maps and the built-up areas were combined with the soil maps. This was done to define the paved areas and assign them a low saturated hydraulic conductivity value so that most water runs off instead of infiltrating into the soil (Wijesekara and Marceau 2012)
	A uniform value of 0.1 m was applied for the entire basin to define the evapotranspiration (ET) surface depth. This parameter corresponds to the thickness of the capillary zone that determines the ET from the unsaturated zone (Wijesekara and Marceau 2012)
Channel flow	The representation of the channel flow is managed by MIKE-11 and is dynamically linked to MIKE SHE. A total of 35 river branches were added to the current river network consisting of main and several minor tributary branches in the upper watershed to help direct the overland flow into the main tributaries and rivers. A total of 353 cross sections were added, which include field surveyed and LiDAR generated cross sections. Surveyed cross sections of the Elbow River and its branches were revised to correct inconsistencies with the topography. 76 surface water extractions (28 seasonal and 48 all season) were included to the existing river network. All upstream unconnected river branches begin at the headwaters of the river network and were set as no-flow boundaries (water is introduced to the streams via overland and baseflow). The downstream boundary of the model was selected as the water level in Glenmore Reservoir. Appropriate value for the riverbed resistance in Manning's M (30.0) and riverbed leakage coefficient, the parameter that regulates the exchange of water between the groundwater and channel flow components of the model ($1e-006$ s^{-1}) were found through sensitivity analysis (DHI Water and Environment 2010, Wijesekara et al. 2012, Wijesekara and Marceau 2012)
Initial groundwater table	In order to setup the initial groundwater table, which played a key role in the calibration of the model, the initial groundwater potential heads needed to be defined for each geological layer. They were derived by running MIKE SHE (from 1961 to 1981) in steady-state mode using a constant, spatially variable recharge, and using a constant water level boundary condition along the river network (DHI Water and Environment 2010)

Fig. 14 (Appendix A): Geological unit distribution of the sand (**a**) and clay/till (**b**) layers. Bedrock is a uniformly distributed constant at the value "4" for the entire area

References

Almeida CM, Gleriani JM, Castejon EF, Soares-Filho BS (2008) Using neural networks and cellular automata for modeling intra-urban land-use dynamics. Int J Geogr Inf Sci 22(9):943–963

AquaResource Inc (2011) Integrated surface and groundwater model review and technical guide. Prepared for Ontario Ministry of Natural Resources. Available at: http://www.google.ca/url?sa=t&rct=j&q=&esrc=s&source=web&cd=1&ved=0CC4QFjAA&url=http%3A%2F%2Fwww.waterbudget.ca%2Fsystem%2Ffiles

%2Fpublications%2F2011_AquaResource_Integratedmodelling
Guide.pdf&ei=wFifUfmKIs7xigKQ0YDAAg&usg=AFQjCNH6
hkXxIzOIf_JJDHu33JPi268nGA

Barredo JI, Kasanko M, McCormick N, Lavalle C (2003) modeling dynamic spatial processes: simulation of urban future scenarios through cellular automata. Landsc Urban Plan 64(3):145–160

Bow River Basin Council (2010) Bow River Basin: State of the watershed summary, Calgary, Alberta. Bow River Basin Council. http://wsow.brbc.ab.ca/reports/BRBCWSOWBookletV2-Dec28.pdf

Chen Z, Grasby SE, Osadetz KG, Fesko P (2006) Historical climate and stream flow trends and future water demand analysis in the Calgary region, Canada. Water Sci Technol 53(10):1–11

Chu HJ, Lin YP, Huang CW, Hsu CY, Chen HY (2010) Modeling the hydrologic effects of dynamic land-use change using a distributed hydrologic model and a spatial land-use allocation model. Hydrol Process 24:2538–2554

Coote DR, Gregorich LJ (2000) The health of our water: towards sustainable agriculture in Canada. Research Branch, Agriculture and Agri-Food Canada, Publication 2020/E. Minister of Public Works and Government Services Canada, Ottawa

DeFries R, Eshleman KN (2004) Land-use change and hydrologic processes: a major focus for the future. Hydrol Process 18:2183–2186

DHI (2009) MIKE SHE. User Manual Volume 2: Reference Guide

DHI Water and Environment (2010) Elbow River watershed hydrologic modeling final report. Report submitted to Alberta Environment

Eiseltová M, Pokorny J, Hesslerová P, Ripl W (2012) Evapotranspiration—a driving force in landscape sustainability. In: Irmak A (ed) Evapotranspiration—remote sensing and modeling. Intech Publisher, pp 305–328

ERWP (2012) Elbow River Watershed Partnership. http://www.erwp.org/

Fohrer N, Haverkamp S, Frede HG (2005) Assessment of the effects of land use patterns on hydrologic landscape functions, development of sustainable land use concepts for low mountain range areas. Hydrol Process 19:659–675

Gan TY (2000) Reducing vulnerability of water resources of Canadian prairies to potential droughts and possible climatic warming. Water Resour Manage 14(2):111–135

Graham DN, Butts MB (2005) Flexible, integrated watershed modeling with MIKE SHE. In: Singh VP, Frevert DK (eds) Watershed models. CRC Press, Boca Raton, pp 245–272

Haith DA, Shoemaker IL (1987) Generalized watershed loading functions for stream flow nutrients. Water Resour Bull 107:121–137

Hasbani J-G (2008) Semi-automated calibration of a cellular automata model to simulate land-use changes in the Calgary region. Unpublished M.Sc. thesis, Department of Geomatics Engineering, University of Calgary, 96 pp

Hasbani J-G, Wijesekara N, Marceau DJ (2011) An interactive method to dynamically create transition rules in a land-use cellular automata model. In: Salcido A (ed) Cellular automata—simplicity behind complexity. InTech. http://www.intechopen.com/books/cellular-automata-simplicity-behind-complexity/an-interactive-method-todynamically-create-transition-rules-in-a-land-use-cellular-automata-model

Hurkmans R, Terink W, Uijlenhoet R, Moors EJ, Troch PA, Verburg PH (2009) Effects of land use changes on stream flow generation in the Rhine basin. Water Resour Res 45:W06405. doi:10.1029/2008WR007574

Intergovernmental Panel on Climate Change (IPCC) (2000) In: Nakicenovic N et al (eds) Special report on emissions scenarios: a special report of working group III of the intergovernmental panel on climate change. Cambridge Univ. Press, Cambridge

Kuusisto E (1980) On the values and variability of degree-day melting factor in Finland. Nord Hydrol 11:235–242

Leaf CF, Brink GE (1973). Hydrologic simulation model of Colorado subalpine forest. U.S. Department of Agriculture, Forest Service Research Paper, RM-107, 23 pp

Li L, Sato Y, Zhu H (2003) Simulating spatial urban expansion based on a physical process. Landsc Urban Plan 64(1–2):67–76

Lin YP, Hong NM, Wu PJ, Wu CF, Verburg PH (2007) Impacts of land use change scenarios on hydrology and land use patterns in the Wu-Tu watershed in Northen Taiwan. Landsc Urban Plan 80(1–2):111–126

Marceau DJ, Wang F, Wijesekara N (2013a) Investigating land-use dynamics at the periphery of a fast-growing city with cellular automata at two spatial scales. In Modeling of land-use and ecological dynamics. Springer Berlin Heidelberg, pp 51–79

Marceau DJ, Wang F, Farjad B, Wijesekara N, Hasbani J-G (2013b) Sensitivity of a cellular automata to historical data used for its calibration and impact on hydrological processes. Annual Meeting of the Association of American Geographers, Los Angeles, April 9–13

Ménard A, Marceau DJ (2007) Simulating the impact of forest management scenarios in an agricultural landscape of southern Quebec, Canada, using a geographic cellular automaton. Landsc Urban Plan 79(3–4):253–265

Moriasi DN, Arnold JG, Van Liew MW, Bingner RL, Harmel RD, Veith TL (2007) Model evaluation guidelines for systematic quantification of accuracy in watershed simulations. Trans ASABE 50(3):885–900

Niehoff D, Fritsch U, Bronstert A (2002) Land-use impacts on storm-runoff generation, scenarios of land-use change and simulation of hydrological response in a meso-scale catchment in SW-Germany. J Hydrol 267(1–2):80–93

Oogathoo S (2006) Runoff simulation in the Canagagigue Creek watershed using the MIKE SHE Model. Unpublished M.Sc. thesis, Department of Bioresource Engineering, Faculty of Agricultural and Environmental Sciences, McGill University, Montreal, Canada, 109 pp

Refsgaard JC (1997) Parameterization, calibration and validation of distributed hydrological models. J Hydrol 198:69–97

Refsgaard JC, Storm B, Clausen T (2010). Système Hydrologique Européen (SHE): review and perspectives after 30 years development in distributed physically-based hydrological modeling. Hydrol Res 41:355–377

Richards JA (2006). Remote sensing digital image analysis: an introduction. Springer, 439 pp

Rocky View County (2012) Rocky view 2060. Growth management strategy, http://www.rockyview.ca/2060/reports/Final_GMS_Document.pdf

Rood SB, Samuelson GM, Weber JK, Wywrot KA (2005) Twentieth-century decline in stream flows from the hydrographic apex of North America. J Hydrol 306(1):215–233

Rood SB, Pan J, Gill KM, Franks CG, Samuelson GM, Shepherd A (2008) Declining summer flows of Rocky Mountain Rivers: changing seasonal hydrology and probable impacts on floodplain forests. J Hydrol 349(3):397–410

Sahoo GB, Ray C, De Carlo EH (2006) Calibration and validation of a physically distributed hydrological model MIKE SHE to predict stream flow at high frequency in a flashy mountainous Hawaii stream. J Hydrol 327(1–2):94–109

Santé I, García AM, Miranda D, Crecente R (2010) Cellular automata models for the simulation of real-world urban processes: a review and analysis. Landsc Urban Plan 96:108–122

Schindler DW, Donahue WF (2005) A case study of the Saskatchewan River system. Rosenburg Conference on Managing Upland Watersheds in an Era of Global Change, Banff, Alberta, 6–11 Sept

Schindler DW, Donahue WF (2006) An impending water crisis in Canada's western prairie provinces. Proc Natl Acad Sci USA 103(19):7210–7216

Scurlock JMO, Asner GP, Gower ST (2001) Worldwide Historical estimates of Leaf Area Index, 1932–2000, DOE Scientific and Technical Information. http://www.osti.gov/bridge/

Shen Z, Kawakami M, Kawamura I (2009) Geosimulation model using geographic automata for simulating land-use patterns in urban partitions. Environ Plan B 36:802–823

Shepherd A, Gill KM, Rood SB (2010) Climate change and future flows of Rocky Mountain rivers: converging forecasts from empirical trend projection and down scaled global circulation modeling. Hydrol Process 24(26):3864–3877

Statistics Canada (2012) 2011 Census Profile, Calgary. http://www12.statcan.gc.ca/census-recensement/index-eng.cfm

Stevens D, Dragicevic S, Rothley K (2007) iCity: A GIS–CA modeling tool for urban planning and decision making. Environ Model Softw 22(6):761–773

Thanapakpawin P, Richey J, Thomas D, Rodda S, Campbell B, Logsdon M (2006) Effects of land use change on the hydrologic regime of the Mae Chaem river basin, NW Thailand. J Hydrol 334:215–230

The City of Calgary (2010) 2010 civic census results. http://www.calgary.ca/CA/city-clerks/Documents/Election-and-information-services/Census/2010_census_result_book.pdf

The City of Calgary (2012) Economic Outlook: 2011–2021, Calgary and Region, vol 2. Calgary Economic Development 2012

Valeo C, Xiang Z, Bouchart FJ-C, Yeung P, Ryan MC (2007) Climate change impacts in the Elbow River watershed. Can Water Resour J 32(4):285–302

Verburg PH, Veldkamp A, Rounsevell MDA (2006) Scenario-based studies of future land use in Europe. Agric Ecosyst Environ 114:1–6

Wang F, Marceau DJ (2013) Simulating land-use changes at a fine spatial scale using a patch-based cellular automata. Trans GIS (in press). 10.1111/tgis.12009

White R, Engelen G (2000) High-resolution integrated modeling of the spatial dynamics of urban and regional systems. Comput Environ Urban Syst 24:383–400

Wijesekara N (2013) An integrated modeling system to simulate the impact of land-use changes on hydrological processes in the Elbow River watershed in Southern Alberta. Unpublished Ph.D. thesis, Department of Geomatics Engineering, University of Calgary, 177 pp

Wijesekara GN, Marceau DJ (2012) Elbow River Watershed MIKE-SHE model: enhancement and scenario modelling project. Report submitted to Dr. Anil Gupta, Alberta Environment, Calgary, AB, Canada

Wijesekara N, Gupta A, Valeo C, Hasbani J-G, Qiao Y, Delaney P, Marceau DJ (2012) Assessing the impact of future land-use changes on hydrological processes in the Elbow River watershed in southern Alberta, Canada. J Hydrol 412–413:220–232

Xiang Z (2004) Physically-based modeling for improved flood prediction in the Elbow River watershed. Unpublished M.Sc. thesis, Department of Civil Engineering, University of Calgary, 236 pp

Yan J, Smith KR (1994) Simulation of integrated surface water and ground water systems - model formulation. Water Resour Bull 30(5):879–890